Table 3. The Baseline and the Change from Baseline to Last Observation Carried Forward in Efficacy End Points

Efficacy End Points by Group	No.	Baseline, Mean±Standard Error	Change from Baseline to Last Observation Carried Forward		
			Mean±Standard Error	*95% Confidence Interval*	*P Value**
Fluorescein corneal staining					
2% Rebamipide	93	7.0±0.2	−3.7±0.3	−4.2 to −3.2	
0.1% Sodium hyaluronate	95	7.0±0.2	−2.9±0.2	−3.2 to −2.5	0.006
Lissamine green conjunctival staining					
2% Rebamipide	93	9.8±0.4	−4.5±0.3	−5.2 to −3.9	
0.1% Sodium hyaluronate	95	10.1±0.4	−2.4±0.3	−2.9 to −1.9	<0.001
Schirmer test					
2% Rebamipide	93	2.5±0.2	0.5±0.2	0.0–1.0	
0.1% Sodium hyaluronate	95	2.3±0.2	1.0±0.3	0.4–1.5	0.229
Tear film break-up time					
2% Rebamipide	93	2.7±0.1	0.8±0.1	0.5–1.1	
0.1% Sodium hyaluronate	95	2.5±0.1	0.6±0.1	0.3–0.8	0.218
Foreign body sensation					
2% Rebamipide	69	2.0±0.1	−1.4±0.1	−1.6 to −1.2	
0.1% Sodium hyaluronate	68	1.8±0.1	−1.0±0.1	−1.1 to −0.8	0.004
Dryness					
2% Rebamipide	76	2.4±0.1	−1.4±0.1	−1.7 to −1.2	
0.1% Sodium hyaluronate	87	2.6±0.1	−1.2±0.1	−1.4 to −1.0	0.139
Photophobia					
2% Rebamipide	62	1.8±0.1	−1.1±0.1	−1.3 to −0.9	
0.1% Sodium hyaluronate	53	1.8±0.1	−0.8±0.1	−1.1 to −0.6	0.127
Eye pain					
2% Rebamipide	50	1.9±0.1	−1.5±0.1	−1.7 to −1.2	
0.1% Sodium hyaluronate	58	1.9±0.1	−1.0±0.1	−1.2 to −0.7	0.014
Blurred vision					
2% Rebamipide	53	1.8±0.1	−1.1±0.1	−1.3 to −0.9	
0.1% Sodium hyaluronate	55	1.9±0.1	−0.9±0.1	−1.1 to −0.6	0.242

**t* test.

TBUT, because disturbance of ocular surface mucin is thought to be one of the main causes of tear film instability and the accompanying shorter TBUT.[1]

There were no significant safety problems associated with rebamipide treatment and the adverse event profile was consistent with previous studies. As in previous trials, the most frequent adverse event was dysgeusia, possibly caused by the bitter taste associated with the active ingredient. However, in Japan, of 10 047 patients with gastric ulcer and gastritis treated by oral formulation of OPC-12759, adverse reactions were reported in 54 patients (0.54%), mainly gastrointestinal symptoms such as constipation, flatulence, nausea, and diarrhea.[19]

Rebamipide ophthalmic suspension does not contain preservatives that can be detrimental to eye health. One of the most commonly used preservatives in ocular products is benzalkonium chloride, which destabilizes the tear film, disrupts the corneal epithelium, decreases the density of goblet cells, and causes conjunctival squamous metaplasia and apoptosis and damage to deeper ocular tissues.[33,34] Such adverse effects are clearly not ideal in a patient with dry eye, particularly if those patients must rely on such products over a long period of time. In fact, the use of preservative-free ocular products is recommended.[34,35] Thus, rebamipide may be expected to be less harmful even if it is used in the long-term.

The efficacy and safety of 2% rebamipide ophthalmic suspension in the short term (4 weeks) was demonstrated in both this study and the phase 2 study.[24] However, long-term treatment would be required for dry eye because it is often seen as a chronic disease. Further studies will be required to

Table 4. Incidence of Adverse Events Observed in at Least 2 Patients in Any Treatment Group

	2% Rebamipide (n = 93)	0.1% Sodium Hyaluronate (n = 95)
Patients with any adverse event	27 (29.0)	19 (20.0)
Ocular events		
Conjunctival hemorrhage	1 (1.1)	2 (2.1)
Eye irritation	0 (0.0)	2 (2.1)
Eye pain	0 (0.0)	3 (3.2)
Visual impairment	2 (2.2)	0 (0.0)
Eye pruritus	4 (4.3)	2 (2.1)
Nonocular events		
Nasopharyngitis	1 (1.1)	2 (2.1)
White blood cell count decreased	3 (3.2)	0 (0.0)
Dysgeusia (bitter taste)	9 (9.7)	0 (0.0)
Headache	2 (2.2)	0 (0.0)

Data are presented as number (%).

investigate whether the improvements reported with rebamipide are maintained in the longer term.

In conclusion, this study showed that a 4-week, 4-times daily treatment with 2% rebamipide was effective in improving the objective signs and subjective symptoms of dry eye. These results suggest that rebamipide may lead to improved treatment of corneal and conjunctival epithelial damage and improvement in symptoms in patients with dry eye. Such efficacy, in addition to the well-tolerated profile of rebamipide, makes it a potentially useful treatment option for dry eye.

References

1. The definition and classification of dry eye disease: report of the Definition and Classification Subcommittee of the International Dry Eye Workshop (2007). Ocul Surf 2007;5:75–92.
2. de Pinho Tavares F, Fernandes RS, Bernardes TF, et al. Dry eye disease. Semin Ophthalmol 2010;25:84–93.
3. Peral A, Dominguez-Godinez CO, Carracedo G, Pintor J. Therapeutic targets in dry eye syndrome. Drug News Perspect 2008;21:166–76.
4. Gayton JL. Etiology, prevalence, and treatment of dry eye disease. Clin Ophthalmol 2009;3:405–12.
5. Friedman NJ. Impact of dry eye disease and treatment on quality of life. Curr Opin Ophthalmol 2010;21:310–6.
6. Gipson IK. The ocular surface: the challenge to enable and protect vision: the Friedenwald lecture. Invest Ophthalmol Vis Sci 2007;48:4390, 4391–8.
7. Shimmura S, Ono M, Shinozaki K, et al. Sodium hyaluronate eyedrops in the treatment of dry eyes. Br J Ophthalmol 1995; 79:1007–11.
8. Aragona P, Di Stefano G, Ferreri F, et al. Sodium hyaluronate eye drops of different osmolarity for the treatment of dry eye in Sjogren's syndrome patients. Br J Ophthalmol 2002;86: 879–84.
9. Condon PI, McEwen CG, Wright M, et al. Double blind, randomised, placebo controlled, crossover, multicentre study to determine the efficacy of a 0.1% (w/v) sodium hyaluronate solution (Fermavisc) in the treatment of dry eye syndrome. Br J Ophthalmol 1999;83:1121–4.
10. American Academy of Ophthalmology Cornea/External Disease Panel. Preferred Practice Pattern Guidelines. Dry Eye Syndrome. Limited revision. San Francisco, CA: American Academy of Ophthalmology; 2011. Available at: http://one.aao.org/CE/PracticeGuidelines/PPP.aspx. Accessed July 26, 2012.
11. Slusser TG, Lowther GE. Effects of lacrimal drainage occlusion with nondissolvable intracanalicular plugs on hydrogel contact lens wear. Optom Vis Sci 1998;75:330–8.
12. Lemp MA. Advances in understanding and managing dry eye disease. Am J Ophthalmol 2008;146:350–6.
13. Corfield AP, Carrington SD, Hicks SJ, et al. Ocular mucins: purification, metabolism and functions. Prog Retin Eye Res 1997;16:627–56.
14. Ralph RA. Conjunctival goblet cell density in normal subjects and in dry eye syndromes. Invest Ophthalmol 1975;14:299–302.
15. Danjo Y, Watanabe H, Tisdale AS, et al. Alteration of mucin in human conjunctival epithelia in dry eye. Invest Ophthalmol Vis Sci 1998;39:2602–9.
16. Argueso P, Balaram M, Spurr-Michaud S, et al. Decreased levels of the goblet cell mucin MUC5AC in tears of patients with Sjogren syndrome. Invest Ophthalmol Vis Sci 2002;43: 1004–11.
17. Shigemitsu T, Shimizu Y, Ishiguro K. Mucin ophthalmic solution treatment of dry eye. Adv Exp Med Biol 2002;506: 359–62.
18. Iijima K, Ichikawa T, Okada S, et al. Rebamipide, a cytoprotective drug, increases gastric mucus secretion in human: evaluations with endoscopic gastrin test. Dig Dis Sci 2009; 54:1500–7.
19. Naito Y, Yoshikawa T. Rebamipide: a gastrointestinal protective drug with pleiotropic activities. Expert Rev Gastroenterol Hepatol 2010;4:261–70.
20. Yamasaki K, Kanbe T, Chijiwa T, et al. Gastric mucosal protection by OPC-12759, a novel antiulcer compound, in the rat. Eur J Pharmacol 1987;142:23–9.
21. Urashima H, Okamoto T, Takeji Y, et al. Rebamipide increases the amount of mucin-like substances on the conjunctiva and cornea in the N-acetylcysteine-treated in vivo model. Cornea 2004;23:613–9.
22. Urashima H, Takeji Y, Okamoto T, et al. Rebamipide increases mucin-like substance contents and periodic acid Schiff reagent-positive cells density in normal rabbits. J Ocul Pharmacol Ther 2012;28:264–70.
23. Takeji Y, Urashima H, Aoki A, Shinohara H. Rebamipide increases the mucin-like glycoprotein production in corneal epithelial cells. J Ocul Pharmacol Ther 2012;28:259–63.
24. Kinoshita S, Awamura S, Oshiden K, et al. Rebamipide (OPC-12759) in the treatment of dry eye: a randomized, double-masked, multicenter, placebo-controlled phase II study. Ophthalmology 2012;119:2471–8.
25. Pocock SJ, Simon R. Sequential treatment assignment with balancing for prognostic factors in the controlled clinical trial. Biometrics 1975;31:103–15.
26. Lemp MA. Report of the National Eye Institute/Industry workshop on Clinical Trials in Dry Eyes. CLAO J 1995;21: 221–32.
27. Schaumberg DA, Dana R, Buring JE, Sullivan DA. Prevalence of dry eye disease among US men: estimates from the Physicians' Health Studies. Arch Ophthalmol 2009;127:763–8.
28. The epidemiology of dry eye disease: report of the Epidemiology Subcommittee of the International Dry Eye WorkShop (2007). Ocul Surf 2007;5:93–107.
29. Hamrah P, Alipour F, Jiang S, et al. Optimizing evaluation of lissamine green parameters for ocular surface staining. Eye (Lond) 2011;25:1429–34.
30. Khanal S, Tomlinson A, McFadyen A, et al. Dry eye diagnosis. Invest Ophthalmol Vis Sci 2008;49:1407–14.
31. Sall K, Stevenson OD, Mundorf TK, Reis BL, CsA Phase 3 Study Group. Two multicenter, randomized studies of the efficacy and safety of cyclosporine ophthalmic emulsion in moderate to severe dry eye disease. Ophthalmology 2000;107: 631–9.
32. Rivas L, Oroza MA, Perez-Esteban A, Murube-del-Castillo J. Morphological changes in ocular surface in dry eyes and other disorders by impression cytology. Graefes Arch Clin Exp Ophthalmol 1992;230:329–34.
33. Burstein NL. The effects of topical drugs and preservatives on the tears and corneal epithelium in dry eye. Trans Ophthalmol Soc U K 1985;104:402–9.
34. Baudouin C, Labbe A, Liang H, et al. Preservatives in eyedrops: the good, the bad and the ugly. Prog Retin Eye Res 2010;29:312–34.
35. Asbell PA. Increasing importance of dry eye syndrome and the ideal artificial tear: consensus views from a roundtable discussion. Curr Med Res Opin 2006;22:2149–57.

Footnotes and Financial Disclosures

Originally received: August 2, 2012.
Final revision: October 24, 2012.
Accepted: November 19, 2012.
Available online: March 13, 2013. Manuscript no. 2012-1169.

[1] Department of Ophthalmology, Kyoto Prefectural University of Medicine, Kyoto, Japan.

[2] Otsuka Pharmaceutical Co, Ltd, Tokyo, Japan.

*A list of members of the Rebamipide Ophthalmic Suspension Phase 3 Study Group is available at http://aaojournal.org.

Presented in part at: Association for Research in Vision and Ophthalmology Annual Meeting, May 2011, Fort Lauderdale, Florida.

Financial Disclosure(s):
The author(s) have made the following disclosure(s):
Shigeru Kinoshita: Consultant—Otsuka Pharmaceutical Co, Ltd.
Kazuhide Oshiden: Employee—Otsuka Pharmaceutical Co, Ltd.
Saki Awamura: Employee—Otsuka Pharmaceutical Co, Ltd.
Hiroyuki Suzuki: Employee—Otsuka Pharmaceutical Co, Ltd.
Norihiro Nakamichi: Employee—Otsuka Pharmaceutical Co, Ltd.
Supported by a grant from Otsuka Pharmaceutical Co, Ltd, Tokyo, Japan.

Correspondence:
Shigeru Kinoshita, MD, PhD, Department of Ophthalmology, Kyoto Prefectural University of Medicine, 465 Kajii-cho, Hirokoji-agaru, Kawaramachi-dori, Kamigyo-ku, Kyoto 602-0841, Japan. E-mail: shigeruk@koto.kpu-m.ac.jp.

Classification of Secondary Corneal Amyloidosis and Involvement of Lactoferrin

Kaoru Araki-Sasaki, MD, PhD,[1] Koji Hirano, MD, PhD,[2] Yasuhiro Osakabe, PhD,[3] Masahiko Kuroda, MD, PhD,[3] Kazuko Kitagawa, MD, PhD,[4] Hiroshi Mishima, MD, PhD,[5] Hiroto Obata, MD, PhD,[6] Masakazu Yamada, MD, PhD,[7] Naoyuki Maeda, MD, PhD,[8] Kohji Nishida, MD, PhD,[8] Shigeru Kinoshita, MD, PhD[9]

Purpose: To classify secondary corneal amyloidosis (SCA) by its clinical appearance, to analyze the demographics of the patients, and to determine the involvement of lactoferrin.

Design: Retrospective, observational, noncomparative, multicenter study.

Participants: Twenty-nine eyes of 29 patients diagnosed with SCA by corneal specialists at 9 ophthalmologic institutions in Japan were studied.

Methods: The clinical appearance of SCA was determined by slit-lamp biomicroscopy and was classified into 3 types. The demographics of the patients, for example, age, gender, and the duration of the basic disease (trichiasis, keratoconus, and unknown), were determined for each clinical type. Surgically excised tissues were stained with Congo red and antilactoferrin antibody. The postoperative prognosis also was determined.

Main Outcome Measures: Clinical appearance of the 3 types of SCA, along with the gender, age, and duration of the basic diseases were determined.

Results: Classification of SCA into 3 types based on clinical appearance found 21 cases with gelatinous drop-like dystrophy (GDLD)-like appearance (GDLD type), 3 cases with lattice corneal dystrophy (LCD)-like appearance (LCD type), and 5 cases with the combined type. Patients with the GDLD type were younger (average age: 40.9 years for the GDLD type, 74.3 years for the LCD type, and 46.8 years for the combined type), predominantly women (85.7% for the GDLD type, 33.3% for the LCD type, and 60% for the combined type), and had the basic disease over a longer time (average duration: 22.1 years for the GDLD type, 14.0 for the LCD type, and 11.4 for the combined type). The distribution of the basic diseases (trichiasis vs. keratoconus vs. unknown) was not significantly different for each type. Surgical treatments, for example, phototherapeutic keratectomy, lamellar keratoplasty, and simple keratectomy, resulted in a good resolution in all surgically treated cases. One subject dropped out of the study. Spontaneous resolution was seen in one subject after epilation of the cilia. Amorphous materials in the excised tissues showed positive staining results by Congo red and by antilactoferrin antibody.

Conclusions: Secondary corneal amyloidosis can be classified into 3 clinical types based on its clinical appearance. Larger numbers of females and lactoferrin expression were seen in all 3 types.

Financial Disclosure(s): The author(s) have no proprietary or commercial interest in any materials discussed in this article. *Ophthalmology 2013;120:1166–1172 © 2013 by the American Academy of Ophthalmology.*

Amyloidosis can develop as a primary or secondary condition in the cornea. Primary amyloidosis is divided into primary localized amyloidosis and primary systemic amyloidosis. Gelatinous drop-like dystrophy (GDLD) and lattice corneal dystrophy (LCD), with the exception of the LCD II type, are examples of primary localized amyloidosis. The LCD II type is a localized form of primary systemic amyloidosis. Localized secondary corneal amyloidosis (SCA) first was described by Stafford and Fine,[1] with its characteristics further defined in later studies.[2–7] Secondary corneal amyloidosis develops after chronic ocular inflammations or corneal disorders, for example, keratoconus, trachoma, phlyctenular keratitis, bullous keratopathy, interstitial keratitis, syphilis, trichiasis, and spheroidal degeneration.[8,9] Because there is a low incidence of this disease, most clinical studies simply have described a single case or, at most, only a few cases in each report.

To diagnose SCA accurately, a histologic examination using Congo red-stained tissues and observation by polarized light microscopy is required. From an ethical point of view, however, the excision of specimens from early-stage cases is not always possible. Therefore, to ensure that an early diagnosis of SCA can be made, it is necessary to establish a standard method that can be used to determine the clinical features of SCA.

It is known that the clinical appearance of SCA can be similar to that of primary corneal amyloidosis, such as GDLD and LCD. The *TACSTD2* gene has been identified as gene responsible for GDLD,[10] whereas the transforming growth factor-β-induced (*TGFBI*) and gelsolin genes are responsible for LCD.[11–14] However, it is still not known why the clinical appearance of SCA resembles primary corneal amyloidosis without the responsible gene mutation. Therefore, analysis of the demographics

ISSN 0161-6420/13/$–see front matter
http://dx.doi.org/10.1016/j.ophtha.2012.11.047

Table 1. Demographics of Each Clinical Type in SCA

Types (n = 29)	Sex (female dominancy)	Age (average: years old)	Duration (years)	Trichiasis: Keratoconus: Unknown
GDLD type (21 cases)	85.7%	40.9	22.1	12:6:3
LCD type (3 cases)	33.3%	74.3	14.0	2:1:0
Combined type (5 cases)	60%	46.8	11.4	3:1:1
Total (SD)	72.4%	45.5 (20.9)	19.6 (13.8)	

GDLD = gelatinous drop-like dystrophy; LCD = lattice corneal dystrophy; SCA = secondary corneal amyloidosis; SD = standard deviation.

of the patients with SCA may provide an answer as to why this occurs.

Lactoferrin was recognized as the precursor protein of SCA by the International Amyloid Committee and was named Alac.[15,16] Thereafter, it was hypothesized that the pathogenesis of SCA may be related to hormonal regulation, with the gender of the subject able to affect the clinical characteristics of SCA. To test this hypothesis, 29 cases of SCA from 9 ophthalmologic institutions in Japan were studied, with SCA classified based on its clinical appearance. The demographics of the patients with SCA then were analyzed.

Patients and Methods

This was a retrospective, observational, noncomparative, multicenter study. Twenty-nine eyes of 29 patients diagnosed with SCA were studied. No subjects demonstrated pathologic changes in the fellow eye, and family history of eye disease was negative in all cases. The examinations and diagnosis were made by corneal specialists at 9 ophthalmologic institutions in Japan. The gender, age, basic clinical findings, duration of symptoms and signs, clinical appearance as determined by slit-lamp examinations, and treatment and prognosis were analyzed.

For the histopathologic analysis, 11 specimens from 29 cases were obtained at keratoplasty, fixed in 10% formaldehyde overnight, and then embedded in paraffin. Then, 3-μm sections were cut and mounted on slides. After deparaffinizing and drying the slides, samples were stained with Congo red. Direct immunohistochemical methods were used to localize lactoferrin in the cornea, as has been described previously in detail.[16] Briefly, sections were incubated with 3% bovine serum albumin at room temperature for 30 minutes to block nonspecific binding. The slides then were incubated with horseradish peroxidase-conjugated rabbit immunoglobulin G fraction against human lactoferrin (no. 55242; Cappel, ICN Pharmaceuticals, Inc, Bryan, OH) for 30 minutes at room temperature. The sections were washed 3 times in phosphate-buffered saline for 10 minutes with 0.02% diaminobenzidine solution, dehydrated through an ethanol series (95% to 70%), and covered with a cover slip using mounting medium. The slides were examined with light and polarizing microscopy.

Informed consent was obtained from all patients. Examination procedures were reviewed by the Institutional Review Board of Ideta Eye Hospital, and the study was conducted in accordance with the tenets of the Declaration of Helsinki.

Results

Classification of Secondary Corneal Amyloidosis

The cases of SCA were classified into 3 types according to their clinical appearances (Fig 1). The GDLD type, which exhibits a clinical appearance similar to that of GDLD, had 1 or more milky-white soft masses on the corneal surface. The LCD type, which exhibits a clinical appearance similar to that of LCD, had fine linear branches that could be detected by scattered scleral illumination. When these types coexisted, for example, a milky-white mass surrounded by lattice-like lines, these corneas were classified as the combined type. Among the 29 cases, 21 were classified as the GDLD type, 3 were classified as the LCD type, and 5 were classified as the combined type. Table 1 summarizes the characteristics of all of the SCA types.

The GDLD-type patients were younger (average age: 40.9 years in the GDLD type, 74.3 years in the LCD type, and 46.8 years in the combined type) and predominantly women (85.7% in the GDLD type, 33.3% in the LCD type, and 60% in the combined type), with the basic diseases shown to be present for a longer time (average age: 22.1 years in the GDLD type, 14.0 years in the LCD type, and 11.4 years in the combined type). For all eyes, the average age of SCA patients was 45.4±20.9 years, with 21 (72.4%) of these 29 SCA cases found in women. No significant differences were noted for the distribution of the basic diseases (trichiasis vs. keratoconus vs. unknown) in each of the clinical types.

In all of the clinical types, the amyloid deposits were located at the corneal area that was inflamed or where the corneal epithelium was irritated continually. In the trichiasis cases, amyloid deposits were seen at the inferior part of the cornea where the eyelid cilia were present. All of the keratoconus cases had worn hard contact lenses for many years, and the amyloid deposits were seen where the contact lenses touched the corneal epithelium at the apex of the cornea. In cases that occurred after penetrating keratoplasty for keratoconus, the amyloid deposits were seen at the edge of the graft where the graft protruded slightly.[17] None of the pathologic regions were found at the limbus.

Prognosis of Secondary Corneal Amyloidosis

Superficial treatments, which included phototherapeutic keratectomy, keratectomy, or lamellar keratoplasty, were performed on 21 of 29 eyes. With a mean follow-up of 31 months, there were no severe recurrences, vessel invasions, infections, or postoperative complications in the surgically treated cases. One patient dropped out and was lost to follow-up, and there was a very slight recurrence in 7 patients. The other 8 cases were followed up conservatively with only lubrication, because the patients reported only a slight foreign body sensation.

Involvement of Lactoferrin in Secondary Corneal Amyloidosis

Histopathologic examination showed that the excised tissue in 11 cases consisted of amorphous eosinophilic material, with all of these tissues showing positive staining results by both Congo red and antilactoferrin antibody (Figs 2 and 3). This material was demonstrated by the apple-green birefringence typical of

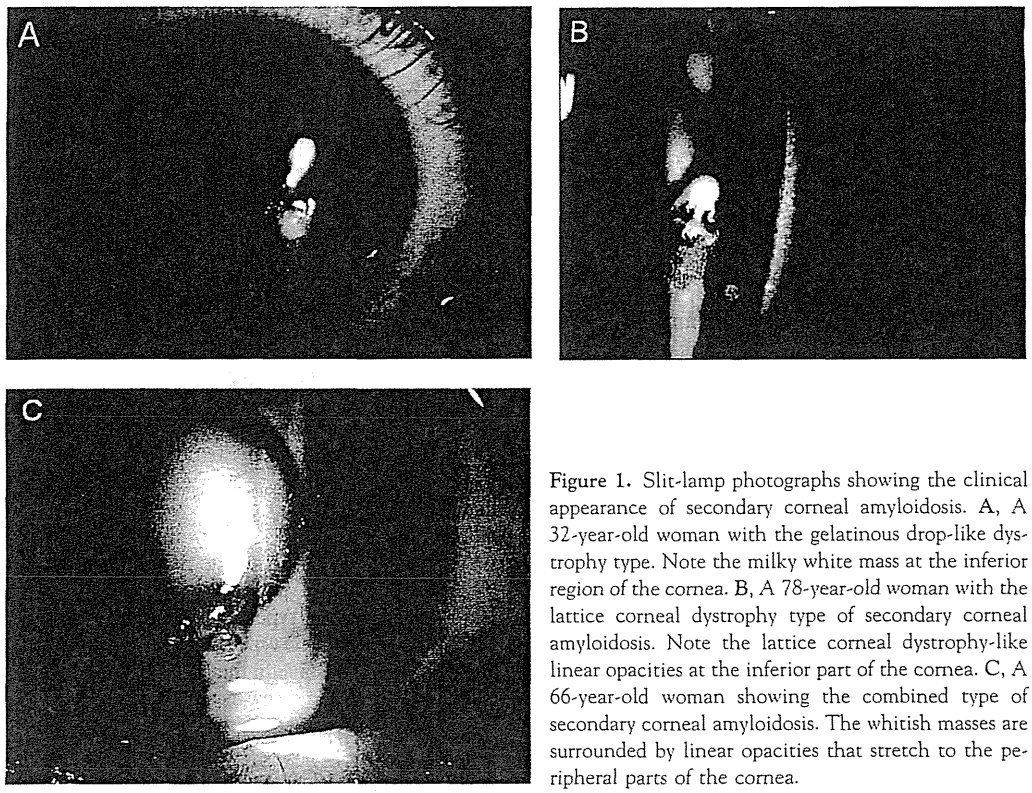

Figure 1. Slit-lamp photographs showing the clinical appearance of secondary corneal amyloidosis. A, A 32-year-old woman with the gelatinous drop-like dystrophy type. Note the milky white mass at the inferior region of the cornea. B, A 78-year-old woman with the lattice corneal dystrophy type of secondary corneal amyloidosis. Note the lattice corneal dystrophy-like linear opacities at the inferior part of the cornea. C, A 66-year-old woman showing the combined type of secondary corneal amyloidosis. The whitish masses are surrounded by linear opacities that stretch to the peripheral parts of the cornea.

amyloid deposits when observed under polarized light (Fig 4). The positive staining areas were located mainly between Bowman's layer and the corneal epithelium. Milky-white masses observed by slit-lamp examination appeared as amorphous material in the epithelial layer, with this material occasionally destroying Bowman's layer, the epithelial layer, or both. The material did not show positive staining with the anti-TGFBI antibody (data not shown).

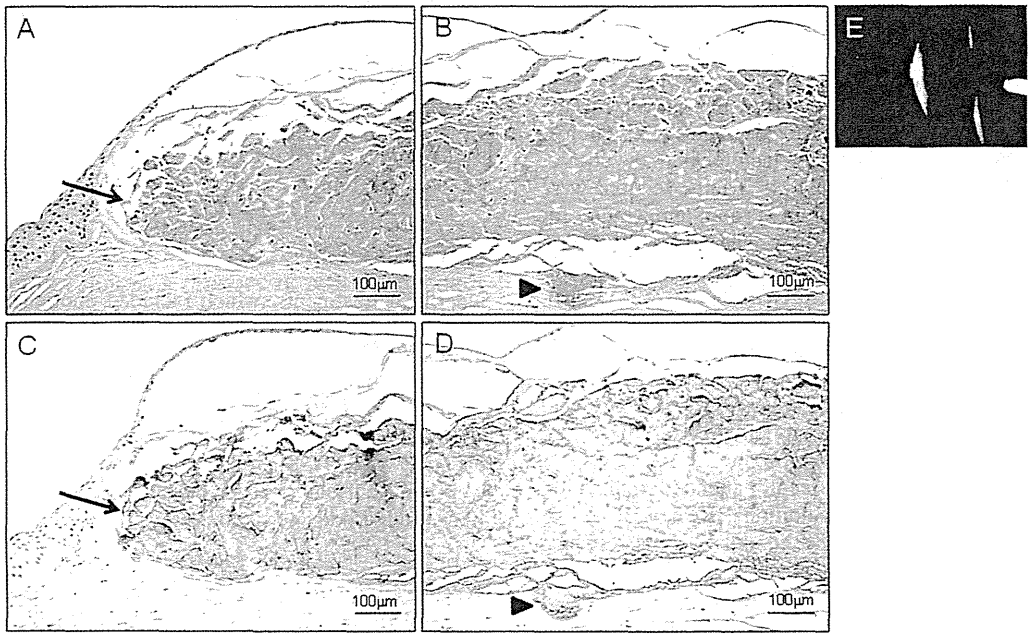

Figure 2. Images showing secondary corneal amyloidosis in a 51-year-old man caused by keratoconus. The tissue obtained during keratectomy was stained with (A, B) Congo red and (C, D) antilactoferrin antibody. A, C, Photomicrographs showing the peripheral region of secondary corneal amyloidosis. B, D, Photomicrographs showing the central region of the cornea. Amorphous eosinophilic material is present between the epithelial layer and Bowman layer (arrow) and shows positive staining results by Congo red and by antilactoferrin antibody. Amorphous materials protrude into the stroma (arrowhead) and totally destroyed the Bowman layer. Note that the epithelial layer is thin and atrophic. E, Slit-lamp photograph.

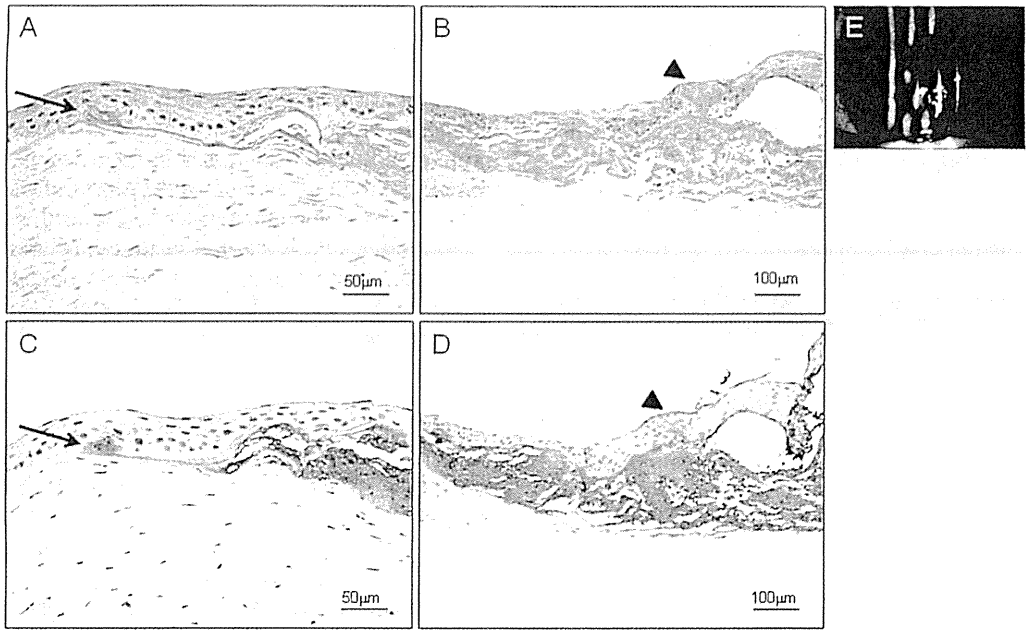

Figure 3. Findings in a 42-year-old man with secondary corneal amyloidosis associated with trichiasis. Amorphous eosinophilic material showed positive staining results by (A, B) Congo red and (C, D) antilactoferrin antibody. A, C, Photomicrographs showing high magnification. B, D, Photomicrographs showing low magnification. Note that the amorphous material is located between the epithelial layer and the Bowman layer (arrow) and the material occupies the epithelial layer (arrowhead). E, Slit-lamp photograph.

Discussion

This study identified characteristic patterns of disease in what is believed to be the first multicenter study of SCA. Because SCA is a rare disease, most of the previously published studies have reported on only a single case or, at most, a few cases at a time. Although a study by Hidayat and Risco[18] was able to examine 62 cases of SCA, unfor-

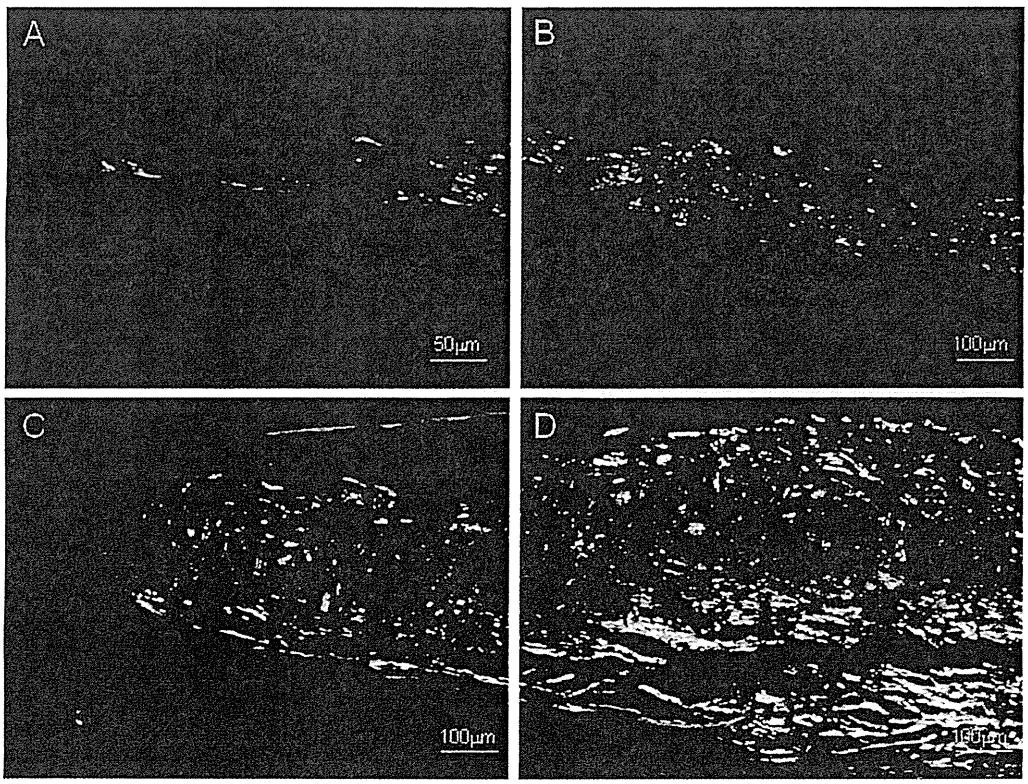

Figure 4. The findings of (A, B) Figure 2A, B and (C, D) Figure and 3A, B under the polarized microscopy. The deposits appear as apple-green birefringence when observed with polarized light.

tunately these cases were limited to those caused by trachoma and there was no classification of the clinical appearances for these patients. The present study collected data on 29 SCA cases that were caused by several basic diseases, with the diagnosis made by corneal specialists from 9 ophthalmologic clinics in Japan.

Secondary corneal amyloidosis can be classified into 3 clinical types based on its clinical appearance, namely, the GDLD type, the LCD type, and the combined type. Originally, GDLD and LCD were defined as belonging to the primary amyloidosis group. Although the original cause is different, SCA and these primary dystrophies (GDLD and LCD) most likely share common pathologic characteristics. Interestingly, patients with the GDLD type of SCA were younger, were predominantly women, and had a longer duration of the basic disease as compared with patients with the other 2 types. However, because the patients were not observed from the point of SCA onset, whether there was transition between these 3 types could not be determined.

These findings indicated a large number of women with SCA, especially in the GDLD-type group. In 2005, Ando et al[15] studied the polymorphism Glu561Asp in patients with SCA and proposed that lactoferrin was the precursor protein of SCA. In an extensive study by Araki-Sasaki et al,[16] this polymorphism was shown to be associated significantly with SCA. A further study also showed that SCA was stained only by the antilactoferrin antibody, and not by antibodies against transthyretin, κ, λ light chain, lysosome, AA, and keratin.[14] Results of in vitro experiments by Nilsson and Dobson[19] suggested that there was aggregation of lactoferrin to form amyloid material. In contrast, Suesskind et al[20] reported finding precipitation of keratoepithelin in eyes with SCA, which suggested that keratoepithelin was the precursor protein of SCA. Therefore, at present it has yet to be proven definitively that lactoferrin is the precursor protein of SCA.

Because Suesskind et al did not stain the specimens with antilactoferrin antibody, the possibility exists that lactoferrin could have played a role in the amyloid formation in their cases. To the contrary, all cases in the present study showed negative staining results for the anti-TGFBI antibody. A complete description of this finding will be shared in an upcoming report. Although preliminary evidence indicates that lactoferrin may be one of the key proteins in SCA, further studies will need to be performed to show definitively that lactoferrin is the precursor protein of SCA.

Klintworth et al[21] suggested that lactoferrin is derived from the tear film in GDLD and that the same may be true in SCA. Another possible origin of lactoferrin has been suggested to be the corneal epithelial cells, which can produce lactoferrin in response to exposure to sex hormones.[22,23] Some may question why a female predominance was seen for SCA but not for GDLD. The authors speculate that there may be differences in unrevealed pathologic events that occur during the very early phase, with these differences ultimately responsible for the variations that are seen for the female predominance in SCA and GDLD. Additionally, after the epithelial breakdown during the late phase, pathologic events such as amyloid extension with lactoferrin from tears very well may be a common event that occurs in both diseases.

Graute-Hernandez et al[24] reported finding a predominance of women patients with Salzmann nodular degeneration of the cornea. Farjo et al[25] also have reported that more than 90% of Salzmann nodular degeneration occurs in females. Stone et al[26] proposed that the increased expression of matrix metalloproteinase-2 and the nodules are the result of chronic epithelial remodeling and wound repair. Thus, SCA and Salzmann nodular degeneration have a common clinical background. Recently, Sundmacher[27] reanalyzed Salzmann's original paper and disclosed that the etiologic postulates were never substantiated by direct observation, but rather were proposed based on indirect histopathologic circumstantial evidence. He revealed that most Salzmann nodules occur without obvious preceding inflammation and discussed that dystrophy and degeneration should be investigated separately with regard to Salzmann degeneration. The entire histologic appearance in Salzmann nodular degeneration seems to be completely different from that seen in SCA, because oxytalan fibers have been identified in the nodular lesions of Salzmann nodular degeneration.[28] However, the pathologic mechanisms associated with SCA and Salzmann nodular degeneration seem to contain common elements to some extent, and this may result in the similarity of clinical features as gray or bluish elevated subepithelial nodules with predominancy in women.

The exact reason why there are 2 forms of SCA, that is, the GDLD type and the LCD type, is still unclear. One possibility is that the region where the amyloid develops may be involved in determining the ultimate clinical appearance. For example, deposits in the epithelial layer may lead to the GDLD type, whereas deposits in the stromal layer could lead to the LCD type. Another possibility is that the lattice appearance could be related to the corneal nerve fibers. Slit-lamp examinations have shown that the lattice appearance often resembles the pattern of myelinated nerve fibers. Although Klintworth[29] demonstrated that amyloid deposits were not associated with the nerve fibers in GDLD, it has been shown that amyloid accumulates in the nerve fibers in cases of familial amyloid polyneuropathy, with transthyretin acting as the precursor protein.[30,31] However, no corneal amyloid deposits were described in familial amyloid polyneuropathy.

A further possibility is that the total amount of aggregated lactoferrin can determine its clinical phenotype. Although the cause of the lattice line has not been determined, the predominance of a younger age and larger numbers of females in the GDLD type suggest that there is a greater production of lactoferrin, aggregated lactoferrin, or both that occurs in the GDLD type versus the LCD type. At present, unfortunately, there is insufficient evidence to prove definitively any of these possibilities. However, the authors speculate that the proportion of nonaggregated mutated precursor protein, aggregated precursor protein, and extended amyloid aggregation may be responsible for determining the ultimate clinical phenotypes seen in SCA. Further investigations will need to be undertaken to clarify why there are 2 amyloid deposit patterns in SCA.

Several studies[32–37] have demonstrated that chronic inflammatory stimulation can be a trigger for the amyloid deposits at the irritated region, for example, at the top of the protruded cornea where the hard contact lens is in contact most tightly with the keratoconic cornea. A previous study has reported that after penetrating keratoplasty was performed in 1 case, the contact lens made a tight contact at the edge of the graft because of astigmatism, with this subsequently leading to SCA in the region.[17] Although the exact mechanism that is involved with the transformation from irritation to amyloid formation has yet to be determined, this previous finding strongly indicates that mechanical irritation seems to be one of the key inducers of amyloid fibril formation during the first stage of inflammation.

In the present cases, there was good prognosis for the surgical treatment of SCAs, with no severe recurrences, vessel invasions, infections, or side effects noted after the procedure. The clinical self-resolution that occurred because of removal of the irritant, for example, extirpation of the eye lashes, suggests that the deposited amyloid may be metabolized. Additionally, the use of therapeutic soft contact lenses is useful in preventing GDLD recurrences after keratoplasty because of the downregulation of the cell metabolism. Thus, the therapeutic effects of SCL may be one method that can be used to prevent the development of SCA.

In summary, this study examined the clinical classifications and demographics of SCA patients. The results showed a predominance of women with SCA, especially the GDLD type, with all cases exhibiting positive staining results for the antilactoferrin antibody. If additional investigations can clarify the mechanism responsible for SCA development, this should provide clues to how to treat this disease successfully in the future.

References

1. Stafford WR, Fine BS. Amyloidosis of the cornea. Arch Ophthalmol 1966;75:53–6.
2. Hayasaka S, Setogawa T, Ohmura M, et al. Secondary localized amyloidosis of the cornea caused by trichiasis. Ophthalmologica 1987;194:77–81.
3. Aldave AJ, Principe AH, Lin DY, et al. Lattice dystrophy-like localized amyloidosis of the cornea secondary to trichiasis. Cornea 2005;24:112–5.
4. Lin PY, Kao SC, Hsueh KF, et al. Localized amyloidosis of the cornea secondary to trichiasis: clinical course and pathogenesis. Cornea 2003;22:491–4.
5. Stern GA, Knapp A, Hood CI. Corneal amyloidosis associated with keratoconus. Ophthalmology 1988;95:52–5.
6. Klemen UM, Kulnig W, Radda TM. Secondary corneal amyloidosis: clinical and pathohistological examinations. Graefes Arch Clin Exp Ophthalmol 1983;220:130–8.
7. Rodrigues M, and Zimmerman LE. Secondary amyloidosis in ocular leprosy. Arch Ophthalmol 1971;85:277–9.
8. Santo RM, Yamaguchi T, Kanai A. Spheroidal keratopathy associated with subepithelial corneal amyloidosis. A clinicopathologic case report and a proposed new classification for spheroidal keratopathy. Ophthalmology 1993;100:1455–61.
9. Trikha S, Sahu D, Jeffry M, Boase D. Secondary corneal amyloidosis in keratoconus. Cornea 2011;30:716–7.
10. Tsujikawa M, Kurahashi H, Tanaka T, et al. Identification of the gene responsible for gelatinous drop-like corneal dystrophy. Nat Genet 1999;21:420–3.
11. Stewart HS, Ridgway AE, Dixon MJ, et al. Heterogeneity in granular corneal dystrophy: identification of three causative mutations in the TGFBI (BIGH3) gene-lessons for corneal amyloidogenesis. Hum Mutat 1999;14:126–32.
12. Stewart H, Black GC, Donnai D, et al. A mutation within exon 14 of the TGFBI (BIGH3) gene on chromosome 5q31 causes an asymmetric, late-onset form of lattice corneal dystrophy. Ophthalmology 1999;106:964–70.
13. Hirano K, Hotta Y, Nakamura M, et al. Late-onset form of lattice corneal dystrophy caused by leu527Arg mutation of the TGFBI gene. Cornea 2001;20:525–9.
14. Gorevic PD, Munoz PC, Gorgone G, et al. Amyloidosis due to a mutation of the gelsolin gene in an American family with lattice corneal dystrophy type II. N Engl J Med 1991;325:1780–5.
15. Ando Y, Nakamura M, Kai H, et al. A novel localized amyloidosis associated with lactoferrin in the cornea. Lab Invest 2002;82:757–65.
16. Araki-Sasaki K, Ando Y, Nakamura M, et al. Lactoferrin Glu561Asp facilitates secondary amyloidosis in the cornea. Br J Ophthalmol 2005;89:684–8.
17. Yamada M, Nishiyama T, Konishi M, et al. Secondary amyloidosis in a corneal graft. Jpn J Ophthalmol 2002;46:305–7.
18. Hidayat AA, Risco JM. Amyloidosis of corneal stroma in patients with trachoma. A clinicopathologic study of 62 cases. Ophthalmology 1989;96:1203–11.
19. Nilsson MR, Dobson CM. In vitro characterization of lactoferrin aggregation and amyloid formation. Biochemistry 2003;42:375–82.
20. Suesskind D, Auw-Haedrich C, Schorderet DF, et al. Keratoepithelin in secondary corneal amyloidosis. Graefes Arch Clin Exp Ophthalmol 2006;244:725–31.
21. Klintworth GK, Valnickova Z, Kielar RA, et al. Familial subepithelial corneal amyloidosis—a lactoferrin-related amyloidosis. Invest Ophthalmol Vis Sci 1997;38:2756–63.
22. Santagati MG, Mule SLT, Amico C, et al. Lactoferrin expression by bovine ocular surface epithelia: a primary cell culture model to study lactoferrin gene promoter activity. Ophthalmic Res 2005;37:270–8.
23. Suzuki T, Kinoshita Y, Tachibana M, et al. Expression of sex steroid hormone receptors in human cornea. Curr Eye Res 2001;22:28–33.
24. Graute-Hernandez EO, Mannis MJ, Eliasieh K, et al. Salzmann nodular degeneration. Cornea 2010;29:283–9.
25. Farjo AA, Halperin GI, Syed N, et al. Salzmann's nodular corneal degeneration clinical characteristics and surgical outcomes. Cornea 2006;25:11–5.
26. Stone DU, Astley RA, Shaver RP, et al. Histopathology of Salzmann nodular corneal degeneration. Cornea 2008;27:148–51.
27. Sundmacher R. Salzmann's nodular degeneration. Mostly an epithelial corneal dystrophy. Ophthalmologe 2012;109:389–403.
28. Obata H, Inoki T, Tsuru T. Identification of oxytalan fibers in Salzmann's nodular degeneration. Cornea 2006;25:586–9.
29. Klintworth GK. Corneal dystrophies Review. Orphanet J Rare Dis 2009;4:7.
30. Nelson GA, Edward DP, Wilensky JT. Ocular amyloidosis and secondary glaucoma. Ophthalmology 1999;106:1363–6.
31. Ando E, Ando Y, Okamura R, et al. Ocular manifestation of familial amyloidotic polyneuropathy type I: long-term follow-up. Br J Ophthalmol 1997;81:295–8.

32. Khalifa YM, Bloomer MM, Margolis TP. Secondary localized sectoral keratoconjunctival amyloidosis from ocular trauma. Cornea 2010;29:1328–9.
33. Hsu HY, Phillips NJ, Harocopos GJ. Secondary amyloidosis in the hydrops lesion of a patient with pellucid marginal degeneration. Cornea 2007;26:992–4.
34. Vemuganti GK, Sridhar MS, Edward DP, et al. Subepithelial amyloid deposits in congenital hereditary endothelial dystrophy: a histopathologic study of five cases. Cornea 2002;21:524–9.
35. Vemuganti GK, Mandal AK. Subepithelial corneal amyloid deposits in a case of congenital glaucoma: a case report. Cornea 2002;21:315–7.
36. Mahmood MA, Teichmann KD. Corneal amyloidosis associated with congenital hereditary endothelial dystrophy. Cornea 2000;19:570–3.
37. Dutt S, Elner VM, Soong HK, et al. Secondary localized amyloidosis in interstitial keratitis. Ophthalmology 1992;99: 817–23.

Footnotes and Financial Disclosures

Originally received: February 26, 2012.
Final revision: November 4, 2012.
Accepted: November 30, 2012.
Available online: February 28, 2013. Manuscript no. 2012-269.

[1] Ideta Eye Hospital, Kumamoto, Japan.

[2] Department of Ophthalmology, Ban Buntane Hotokukai Hospital, Fujita Health University, Nagoya, Japan.

[3] Department of Molecular Pathology, Tokyo Medical University, Tokyo, Japan.

[4] Department of Ophthalmology, Kanazawa Medical University, Kanazawa, Japan.

[5] Department of Ophthalmology, Nara Hospital, Kinki University School of Medicine, Nara, Japan.

[6] Department of Ophthalmology, Jichi Medical University, Tochigi, Japan.

[7] National Institute of Sensory Organs, National Hospital Organization Tokyo Medical Center, Tokyo, Japan.

[8] Department of Ophthalmology, Osaka University Medical School, Osaka, Japan.

[9] Department of Ophthalmology, Kyoto Prefectural University of Medicine, Kyoto, Japan.

Financial Disclosure(s):
The author(s) have no proprietary or commercial interest in any materials discussed in this article.

Correspondence:
Kaoru Araki-Sasaki, MD, PhD, Ideta Eye Hospital, 27 Nishi-Tojincho, Kumamoto City, Kumamoto 860-0035, Japan. E-mail: sasakis@sa2.so-net.ne.jp.

PLOS ONE

Inhibition of TGF-β Signaling Enables Human Corneal Endothelial Cell Expansion *In Vitro* for Use in Regenerative Medicine

Naoki Okumura[1,2], EunDuck P. Kay[1], Makiko Nakahara[1], Junji Hamuro[2], Shigeru Kinoshita[2], Noriko Koizumi[1]*

1 Department of Biomedical Engineering, Faculty of Life and Medical Sciences, Doshisha University, Kyotanabe, Japan, **2** Department of Ophthalmology, Kyoto Prefectural University of Medicine, Kyoto, Japan

Abstract

Corneal endothelial dysfunctions occurring in patients with Fuchs' endothelial corneal dystrophy, pseudoexfoliation syndrome, corneal endotheliitis, and surgically induced corneal endothelial damage cause blindness due to the loss of endothelial function that maintains corneal transparency. Transplantation of cultivated corneal endothelial cells (CECs) has been researched to repair endothelial dysfunction in animal models, though the *in vitro* expansion of human CECs (HCECs) is a pivotal practical issue. In this study we established an optimum condition for the cultivation of HCECs. When exposed to culture conditions, both primate and human CECs showed two distinct phenotypes: contact-inhibited polygonal monolayer and fibroblastic phenotypes. The use of SB431542, a selective inhibitor of the transforming growth factor-beta (TGF-β) receptor, counteracted the fibroblastic phenotypes to the normal contact-inhibited monolayer, and these polygonal cells maintained endothelial physiological functions. Expression of ZO-1 and Na^+/K^+-ATPase maintained their subcellular localization at the plasma membrane. Furthermore, expression of type I collagen and fibronectin was greatly reduced. This present study may prove to be the substantial protocol to provide the efficient *in vitro* expansion of HCECs with an inhibitor to the TGF-β receptor, and may ultimately provide clinicians with a new therapeutic modality in regenerative medicine for the treatment of corneal endothelial dysfunctions.

Citation: Okumura N, Kay EP, Nakahara M, Hamuro J, Kinoshita S, et al. (2013) Inhibition of TGF-β Signaling Enables Human Corneal Endothelial Cell Expansion *In Vitro* for Use in Regenerative Medicine. PLoS ONE 8(2): e58000. doi:10.1371/journal.pone.0058000

Editor: Che John Connon, University of Reading, United Kingdom

Received November 5, 2012; **Accepted** January 29, 2013; **Published** February 25, 2013

Funding: The work was supported in part by the Highway Program for realization of regenerative medicine (Kinoshita and Okumura); http://www.mext.go.jp/english/; and the Funding Program for Next Generation World-Leading Researchers from the Cabinet Office in Japan (Koizumi: LS117); http://www.jsps.go.jp/english/e-jisedai/index.html. The funders had no role in study design, data collection and analysis, decision to publish, or preparation of the manuscript.

Competing Interests: The authors have declared that no competing interests exist.

* E-mail: nkoizumi@mail.doshisha.ac.jp

Introduction

Corneal endothelial dysfunction is a major cause of severe visual impairment leading to blindness due to the loss of endothelial function that maintains corneal transparency. Restoration to clear vision requires either full-thickness corneal transplantation or endothelial keratoplasty. Recently, highly effective surgical techniques to replace corneal endothelium [e.g., Descemet's stripping automated endothelial keratoplasty (DSAEK) and Descemet's membrane endothelial keratoplasty (DMEK)] have been developed [1–3] that are aimed at replacing penetrating keratoplasty for overcoming pathological dysfunctions of corneal endothelial tissue. At present, our group and several other research groups have focused on the establishment of new treatment methods suitable for a practical clinical intervention to repair corneal endothelial dysfunctions [4–9]. Since corneal endothelium is composed of a monolayer and is a structurally flexible cell sheet, corneal endothelial cells (CECs) have been cultured on substrates including collagen sheets, amniotic membrane, or human corneal stroma. Then the cultured CECs are transplanted as a cell sheet. However, these techniques require the use of an artificial or biological substrate that may introduce several problems such as substrate transparency, detachment of the cell sheet from the cornea, and technical difficulty of transplantation into the anterior chamber. In our effort to overcome those substrate-related problems, we previously demonstrated that the transplantation of cultivated CECs in combination with a Rho kinase (ROCK) inhibitor enhanced the adhesion of injected cells onto the recipient corneal tissue without the use of a substrate and successfully achieved the recovery of corneal transparency in two corneal-endothelial-dysfunction animal models (rabbit and primate) [10,11].

However, in the context of the clinical setting, another pivotal practical issue is the *in vitro* expansion of human CECs (HCECs). HCECs are vulnerable to morphological fibroblastic change under normal culture conditions. Although HCECs can be cultivated into a normal phenotype maintaining the contact-inhibited polygonal monolayer, they eventually undergo massive endothelial-mesenchymal transformation after long-term culture or subculture. Thus, cultivation of HCECs with normal physiological function is difficult, yet not impossible [12,13].

Epithelial mesenchymal transformation (EMT) has been well characterized in epithelial-to-mesenchymal transition, and transforming growth factor-beta (TGF-β) can initiate and maintain EMT in a variety of biological and pathological systems [14,15].

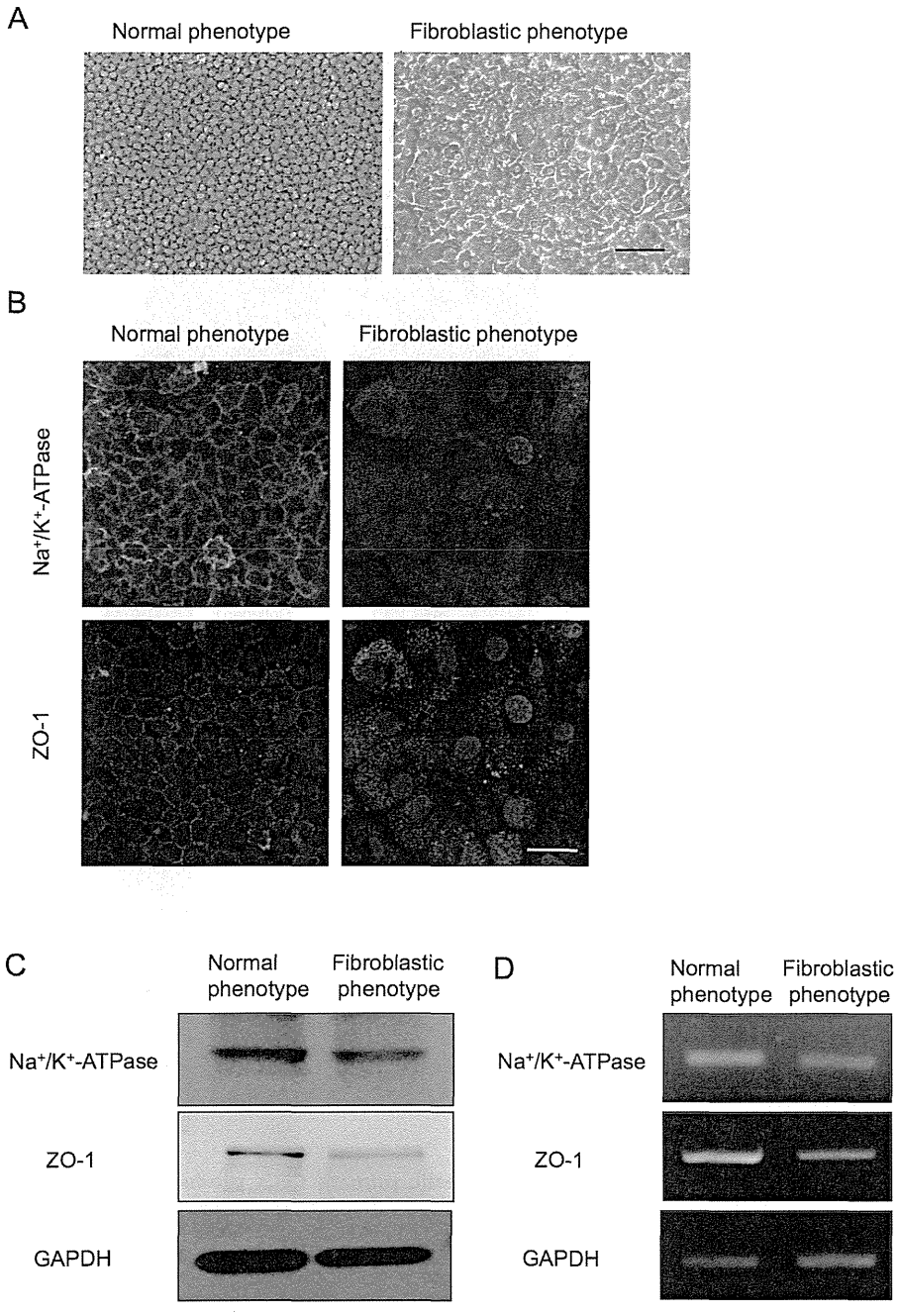

Figure 1. Primate corneal endothelial cells exhibit fibroblastic phenotype and lose functions during cell culture. (A) Cultivated primate CECs demonstrated two distinctive phenotypes; the cells maintained the characteristic polygonal cell morphology and contact-inhibited phenotype (normal phenotype) and the cells showed a fibroblastic cell shape with multi-layering (fibroblastic phenotype). Both phenotypes of the cultured CECs were primary cultured cells. Scale bar: 50 μm. The experiment was performed in triplicate. (B) Na^+/K^+-ATPase and ZO-1 at the plasma membrane was preserved in the normal phenotype, while fibroblastic phenotype completely lost the characteristic staining profile of Na^+/K^+-ATPase and ZO-1 at the plasma membrane. Scale bar: 100 μm. (C+D) Expression of the Na^+/K^+-ATPase and ZO-1 was higher in normal phenotypes than in the fibroblastic phenotypes at both the protein and mRNA levels. Samples were prepared in duplicate. Immunoblotting and semiquantitative PCR were performed in duplicate.
doi:10.1371/journal.pone.0058000.g001

The cellular activity of TGF-β is of particular interest in epithelial cells, as it inhibits the G1/S transition of the cell cycle in these cells. However, the same growth factor is the key signaling molecule for EMT, and the role of TGF-β as a key molecule in the development and progression of EMT is well studied [14–17]. Smad2/3 are signaling molecules downstream of cell-surface receptors for TGF-β in epithelial-to-mesenchymal transition [16,17]. Similar to epithelial cells, TGF-β inhibits the G1/S transition of the cell cycle in CECs [18,19], however, it is not known how TGF-β develops endothelial to mesenchymal transformation and maintains it in CECs. Endothelial-mesenchymal transformation is observed among corneal endothelial dysfunctions such as Fuchs' endothelial corneal dystrophy, pseudoexfoliation syndrome, corneal endotheliitis, surgically-induced corneal

endothelial damage, and corneal trauma and it induces the fibroblastic transformation of CECs [20–23], suggesting that CECs have the biological potential to acquire endothelial to mesenchymal transformation. The apparent presence of fibroblastic phenotypes in primate CECs and HCECs in culture led us to search for the cause of such phenotypic changes of the cultivated cells and for a means in which to prevent such undesirable cellular changes toward endothelial-mesenchymal transformation.

In the present study, we established primate CEC and HCEC cultures which respectively showed two distinctive phenotypes: 1) normal and 2) fibroblastic. We further characterized the two phenotypes and showed evidence that the use of an inhibitor to TGF-β receptor or BMP-7 abolished the fibroblastic phenotypes of cultivated CECs. Thus, intervention by inhibiting the endothelial to mesenchymal transformation process that occurs during the cultivation of CECs will certainly enable the *in vitro* expansion of cultivated HCECs with a normal phenotype which would be ideal for therapeutic clinical application.

Materials and Methods

Ethics Statement

The monkey tissue used in this study was handled in accordance with the ARVO Statement for the Use of Animals in Ophthalmic and Vision Research. The isolation of the tissue was approved by an institutional animal care and use committee of the Nissei Bilis Co., Ltd. (Otsu, Japan) and the Eve Bioscience, Co., Ltd. (Hashimoto, Japan). The human tissue used in this study was handled in accordance with the tenets set forth in the Declaration of Helsinki. A written consent was acquired from the next of kin of all deceased donors regarding eye donation for research. All tissue is recovered under the tenants of the Uniform Anatomical Gift Act (UAGA) of the particular state where the donor was consented and recovered.

Monkey cornea tissues and Research-grade human cornea tissues

Eight corneas from 4 cynomolgus monkeys (3 to 5 years-of-age; estimated equivalent human age: 5 to 20 years) housed at Nissei Bilis and the Keari Co., Ltd., Osaka, Japan, respectively, were used for the MCECs culture. The cynomolgus monkeys were housed in individual stainless steel cages at Nissei Bilis and Eve Bioscience. Each cage was provided with reverse-osmosis water delivered by an automatic water supply system and supplied with experimental animal diet (PS-A; Oriental Yeast Co., Ltd., Tokyo, Japan). Room temperature was controlled by heating units inside the rooms and was maintained at 18.0–26.0°C. The humidity was maintained at 29.5 to 80.4%. Animals were maintained on a 12:12-h light:dark cycle (lights on, 7 a.m. to 19 p.m.). For other research purposes, the animals were given an overdose of intravenous pentobarbital sodium for euthanatization. The corneas of cynomolgus monkeys were harvested after confirmation of cardiopulmonary arrest by veterinarians, and then provided for our research. Twenty human donor corneas were obtained from the SightLife™ (Seattle, WA) eye bank, and all corneas were stored at 4°C in storage medium (Optisol; Chiron Vision Corporation, Irvine, CA) for less than 14 days prior to the primary culture.

Cell culture of monkey CECs (MCECs)

The MCECs were cultivated in modified protocol as described previously [7,24]. Briefly, the Descemet's membrane including CECs was stripped and digested at 37°C for 2 h with 1 mg/mL collagenase A (Roche Applied Science, Penzberg, Germany). After a digestion at 37°C, the MCECs obtained from individual corneas were resuspended in culture medium and plated in 1 well of a 6-well plate coated with FNC Coating Mix® (Athena Environmental

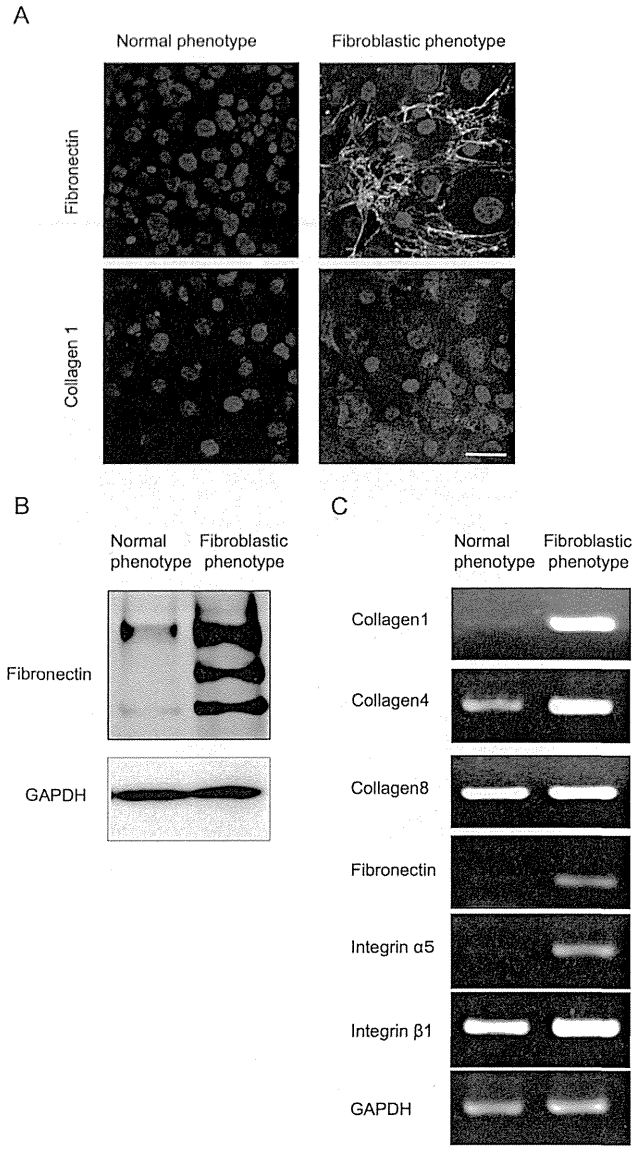

Figure 2. Fibroblastic primate CECs produced an abnormal extra cellular matrix. (A) The fibroblastic phenotype demonstrated excessive ECMs such as fibronectin and collagen type 1, while the normal phenotype completely lost the staining potential. Scale bar: 100 μm. (B) The protein expression level of fibronectin was more strongly upregulated in the fibroblastic phenotype than in the normal phenotype. (C) Semiquantitative PCR analysis showed that the type I collagen transcript [α1(I) mRNA] was abundantly expressed in the fibroblastic phenotypes, while the expression of α1(I) mRNA was reduced in the normal phenotypes. The basement membrane collagen phenotype α1(IV) mRNA was expressed both in normal and fibroblastic phenotypes, yet to a lesser degree in the normal phenotype. Collagen phenotype α1(VIII) mRNA was expressed in both phenotypes at similar levels. Fibronectin and integrin α5 mRNA was observed in the fibroblastic phenotypes, as opposed to the normal phenotypes in which the two transcripts were not expressed. β1 integrin mRNA was expressed in both phenotypes at similar levels. Samples were prepared in duplicate. Immunoblotting and semiquantitative PCR were performed in duplicate.
doi:10.1371/journal.pone.0058000.g002

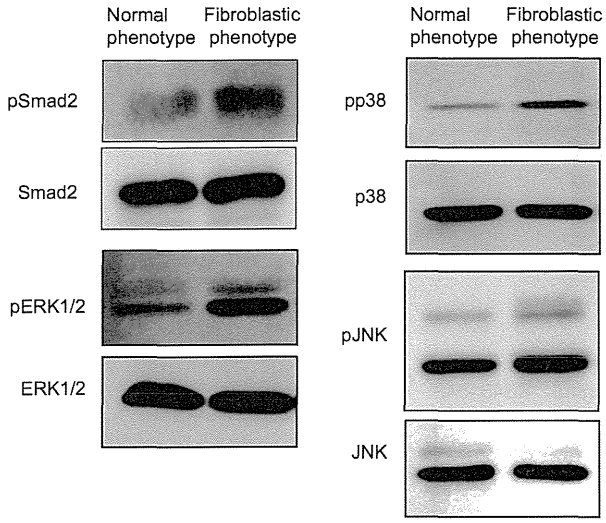

Figure 3. Different activation pattern of fibroblastic change associated pathways in the fibroblastic phenotype of primate CECs. Phosphorylation of Smad2, p38MAPK, and ERK1/2 was promoted in the fibroblastic phenotype compared to that in the normal phenotype, while phosphorylation of JNK was negligible. Samples were prepared in duplicate, and immunoblotting was performed in duplicate.
doi:10.1371/journal.pone.0058000.g003

Sciences, Inc., Baltimore, MD). All primary cell cultures and serial passages of the MCECs were performed in growth medium composed of Dulbecco's modified Eagle's medium (Invitrogen Corporation, Carlsbad, CA) supplemented with 10% fetal bovine serum (FBS), 50 U/mL penicillin, 50 μg/mL streptomycin, and 2 ng/mL FGF-2 (Invitrogen). The MCECs were then cultured in a humidified atmosphere at 37°C in 5% CO_2, and the culture medium was changed every 2 days. When the MCECs reached confluency in 10 to 14 days, they were rinsed in Ca^{2+} and Mg^{2+}-free Dulbecco's phosphate-buffered saline (PBS), trypsinized with 0.05% Trypsin-EDTA (Invitrogen) for 5 min at 37°C, and passaged at ratios of 1:2–4. Cultivated MCECs at passages 2 through 5 were used for all experiments. SB431542 (Merck Millipore, Billerica, MA), a selective inhibitor of transforming growth factor-β (TGF-beta), was tested for the anti-fibroblastic effect.

Cell culture of HCECs

The HCECs were cultivated in a modified version of the protocol used for the MCECs. Briefly, the Descemet's membrane including CECs was stripped and digested at 37°C for 2 h with 1 mg/mL collagenase A (Roche Applied Science). After a digestion at 37°C, the HCECs obtained from individual corneas were resuspended in culture medium and plated in 1 well of a 12-well plate coated with FNC Coating Mix®. The culture medium was prepared according to published protocols [25], but with some modifications. Briefly, basal culture medium containing Opti-MEM-I (Invitrogen), 8% FBS, 5 ng/mL epidermal growth factor (EGF) (Sigma-Aldrich Co., St. Louis, MO), 20 μg/mL ascorbic acid (Sigma-Aldrich), 200 mg/L calcium chloride (Sigma-Aldrich), 0.08% chondroitin sulfate (Wako Pure Chemical Industries, Ltd., Osaka, Japan), and 50 μg/mL of gentamicin was prepared, and the conditioned medium was then recovered after cultivation of inactivated 3T3 fibroblasts. Inactivation of the 3T3 fibroblasts was performed as described previously [26,27]. Briefly, confluent 3T3 fibroblasts were incubated with 4 μg/mL mitomycin C (MMC) (Kyowa Hakkko Kirin Co., Ltd., Tokyo, Japan) for 2 h at 37°C under 5% CO_2, and then trypsinized and plated onto plastic dishes at the density of 2×10^4 cells/cm^2. The HCECs were cultured in a humidified atmosphere at 37°C in 5% CO_2, and the culture medium was changed every 2 days. When the HCECs reached confluency in 14 to 28 days, they were rinsed in Ca^{2+} and Mg^{2+}-free PBS, trypsinized with 0.05% Trypsin-EDTA for 5 min at 37°C, and passaged at ratios of 1:2. Cultivated HCECs at passages 2 through 5 were used for all experiments. To test the anti-fibroblastic effect, the cultured HCECs were passaged at the ratio of 1:2 with medium supplemented with or without SB431542 (0.1, 1, and 10 μM) (Merck Millipore), a neutralizing antibody to TGF-β (500 ng/ml) (R&D Systems, Inc., Minneapolis, MN), Smad3 inhibitor (3 mM) (Merck Millipore), and bone morphogenetic protein (BMP) BMP-7 (10, 100, and 1000 ng/ml) (R&D Systems), and were then evaluated after 1 week.

Histological examination

For histological examination, cultured MCECs or HCECs on Lab-Tek™ Chamber Slides™ (NUNC A/S, Roskilde, Denmark) were fixed in 4% formaldehyde for 10 min at room temperature (RT) and incubated for 30 min with 1% bovine serum albumin (BSA). To investigate the phenotype of the CECs, immunohistochemical analyses of ZO-1 (Zymed Laboratories, Inc., South San Francisco, CA), a tight junction associated protein, Na^+/K^+-ATPase (Upstate Biotechnology, Inc., Lake Placid, NY), the protein associated with pump function, fibronectin (BD, Franklin Lakes, NJ), and actin were performed. ZO-1 and Na^+/K^+-ATPase were used as function related markers of the CECs, fibronectin and collagen type 1 were used to evaluate the fibroblastic change, and actin staining was used to evaluate the cellular morphology. The ZO-1, Na^+/K^+-ATPase, collagen type 1, and fibronectin staining were performed with a 1:200 dilution of ZO-1 polyclonal antibody, Na^+/K^+-ATPase monoclonal antibody, and fibronectin monoclonal antibody, respectively. For the secondary antibody, a 1:2000 dilution of Alexa Fluor® 488-conjugated or Alexa Fluor® 594-conjugated goat anti-mouse IgG (Invitrogen) was used. Actin staining was performed with a 1:400 dilution of Alexa Fluor® 488-conjugated phalloidin (Invitrogen). Cell nuclei were then stained with DAPI (Vector Laboratories, Inc., Burlingame, CA) or propidium iodide (PI) (Sigma-Aldrich). The slides were then inspected by fluorescence microscopy (TCS SP2 AOBS; Leica Microsystems, Wetzlar, Germany). The percentages of Na^+/K^+-ATPase- and ZO-1-positive cells that expressed Na^+/K^+-ATPase and ZO-1 at the plasma membrane in the *in vivo* condition were counted by a blinded examiner.

Immunoblotting

For immunoblotting, the cells were washed with PBS and then lysed with radio immunoprecipitation assay (RIPA) buffer (Bio-Rad Laboratories, Hercules, CA) containing Phosphatase Inhibitor Cocktail 2 (Sigma-Aldrich) and Protease Inhibitor Cocktail (Nacalai Tesque, Kyoto, Japan). The lysates were then centrifuged at 15,000 rpm for 10 min at 4°C. The resultant supernatant was collected and the protein concentration of the sample was assessed with the BCA™ Protein Assay Kit (Takara Bio Inc., Otsu, Japan). The proteins were then separated by sodium dodecyl sulfate polyacrylamide gel electrophoresis (SDS-PAGE) and transferred to polyvinylidene fluoride (PVDF) membranes. The membranes were then blocked with 3% non-fat dry milk (Cell Signaling Technology, Inc., Danvers, MA) in TBS-T buffer. The incubations were then performed with the following primary antibodies: Na^+/K^+-ATPase (Merck Millipore), ZO-1, GAPDH (Abcam, Cambridge, UK), fibronectin, and Smad2 (Cell Signaling Technology),

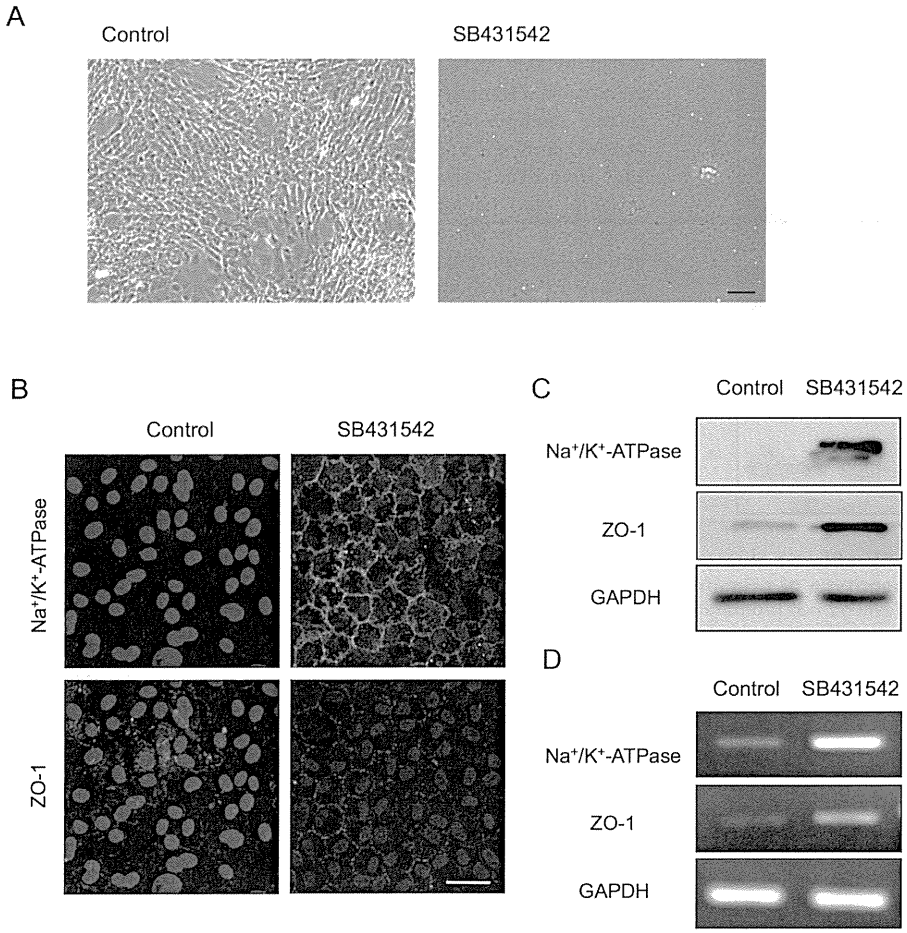

Figure 4. Inhibition of the TGF-β pathway suppressed fibroblastic change and maintained functions. (A) Primate CECs cultured with SB431542 exhibited the authentic polygonal cell shape and contact-inhibited monolayer, while the control CECs exhibited the fibroblastic morphology. Scale bar: 50 μm. (B) SB431542-treated CECs showed the characteristic plasma membrane staining of Na^+/K^+-ATPase and ZO-1, while the control CECs lost their staining. Scale bar: 100 μm. (C+D) Expression of Na^+/K^+-ATPase and ZO-1 was greatly upregulated in the SB431542-treated fibroblastic phenotypes at both the protein and mRNA levels. Samples were prepared in duplicate. Immunoblotting and semiquantitative PCR were performed in duplicate.
doi:10.1371/journal.pone.0058000.g004

phosphorylated Smad2 (Cell Signaling Technology), ERK1/2 (BD), phosphorylated ERK1/2 (BD), p38MAPK (BD), phosphorylated p38MAPK (BD) JNK (BD) or phosphorylated JNK (BD) (1:1000 dilution), and HRP-conjugated anti-rabbit or anti-rabbit IgG secondary antibody (Cell Signaling Technology) (1:5000 dilution). Membranes were exposed by ECL Advance Western Blotting Detection Kit (GE Healthcare, Piscataway, NJ), and then examined by use of the LAS4000S (Fujifilm, Tokyo, Japan) imaging system.

Semiquantitative reverse transcriptase polymerase chain reaction (RT-PCR) and quantitative PCR

Total RNA was extracted from CECs and cDNA was synthesized by use of ReverTra Ace® (Toyobo, Osaka, Japan), a highly efficient RT. The same amount of cDNA was amplified by PCR (GeneAmp 9700; Applied Biosystems) and the following primer pairs: GAPDH mRNA, forward (5′-GAGTCAACGGATTTGGTCGT-3′), and reverse (5′-TTGATTTTGGAGGGATCTCG-3′); Na^+/K^+-ATPase mRNA, forward (5′-CTTCCTCCGCATTTATGCTCATTTTCTCACCC-3′), and reverse (5′-GGATGATCATAAACTTAGCCTTGATGAACTC-3′); ZO-1 mRNA, forward (5′-GGACGAGGCATCATCCCTAA-3′), and reverse (5′-CCAGCTTCTCGAAGAACCAC-3′); collagen1 mRNA, forward (5′-TCGGCGAGAGCATGACCGATGGAT-3′), and reverse (5′-GACGCTGTAGGT GAAGCGGCTGTT-3′); collagen4 mRNA, forward (5′-AGCAAGGTGTTACAGGATTGGT -3′), and reverse (5′- AGAAGGACACTGTGGGTCATCT -3′); collagen8 mRNA, forward (5′-ATGTGATGGCTGTGCTGCTGCTGCCT -3′), and reverse (5′-CTCTTGGGCCAGGCTCTCCA-3′); fibronectin mRNA, forward (5′-AGATGAGTGGGAACGAATGTCT -3′), and reverse (5′-GAGGGTCACACTTGAATTCTCC -3′); integrin α5 mRNA, forward (5′-TCCTCAGCAAGAATCTCAACAA -3′), and reverse (5′-GTTGAGTCCCGTAACTCTGGTC -3′); integrin β1 mRNA, forward (5′-GCTGAAGACTATCCCATTGACC -3′), and reverse (5′-ATTTCCAGATATGCGCTGTTTT -3′). PCR products were analyzed by agarose gel electrophoresis. Quantitative PCR was performed using the following TaqMan® (Invitrogen) primers: collegen1, Hs00164004_m1; fibronectin, Hs01549976_m1; GAPDH, Hs00266705_g1. The PCR was performed using the StepOne™ (Applied Biosystems) real-time PCR system. GAPDH was used as an internal standard.

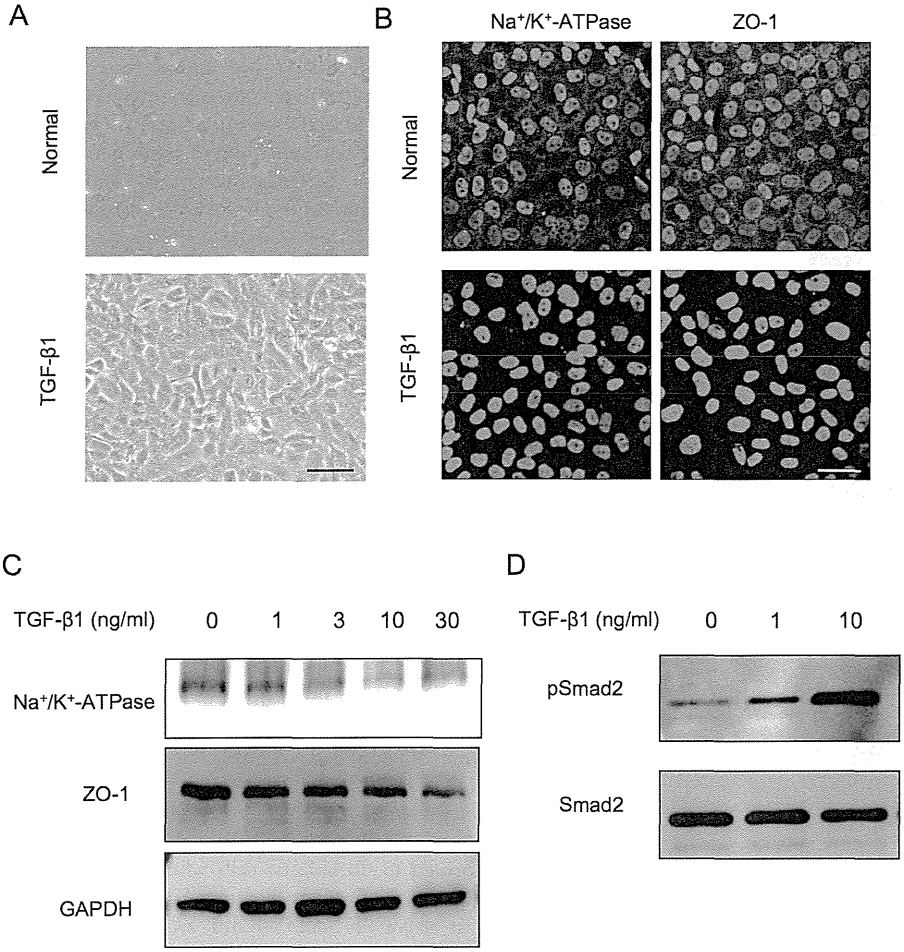

Figure 5. TGFβ induced fibroblastic change and function loss through the activation of the Smad signaling pathways. (A) Normal phenotype primate CECs were transformed to fibroblastic cells when exposed to the exogenous TGF-β1 (10 ng/ml). Scale bar: 50 μm. (B) The staining pattern of Na^+/K^+-ATPase and ZO-1 at the plasma membrane of the normal phenotypes was greatly reduced upon exposure to TGF-β1 (10 ng/ml). Scale bar: 100 μm. (C) TGF-β1 reduced the expression of Na^+/K^+-ATPase and ZO-1 at protein levels dose-dependently. (D) Phosphorylation of Smad2 was increased in a concentration-dependent manner. Samples were prepared in duplicate, and immunoblotting was performed in duplicate.
doi:10.1371/journal.pone.0058000.g005

Enzyme-linked immunosorbent assay (ELISA)

Collagen type I of culture medium supernatant of HCECs were measured using ELISA kits for Collagen Type I Alpha 2 (COL1a2) (Uscn Life Science Inc., Wuhan, China) according to the manufacturer's instructions. Culture medium supernatant from HCECs cultured with or without SB431542 were used for each group (n = 5).

Statistical analysis

The statistical significance (*P*-value) in mean values of the two-sample comparison was determined by use of the Student's t-test. The statistical significance in the comparison of multiple sample sets was analyzed by use of the Dunnett's multiple-comparisons test. Values shown on the graphs represent the mean ± SE.

Results

Two distinct phenotypes of primate CECs during cell culture

Of great interest, the primate CECs in culture demonstrated two distinctive phenotypes when determined by cell morphology and the characteristic contact-inhibited phenotype. Although to culture primate CECs in a normal phenotype while maintaining the monolayer contact-inhibited morphology is possible, they often showed morphological fibroblastic change after primary culture following isolation from the cornea, or long-term culture or subculture, if they were once primary cultured in normal morphology (Fig. 1A). The two phenotypes were then tested for the endothelial characteristics; the staining pattern of Na^+/K^+-ATPase and ZO-1 at the plasma membrane was well preserved in the normal phenotypes, yet the fibroblastic phenotypes completely lost the characteristic staining profile of Na^+/K^+-ATPase and ZO-1 at the plasma membrane (Fig. 1B). Expression of the two functional proteins was found to be much greater in the normal phenotypes than in the fibroblastic phenotypes at both the protein (Fig. 1C) and mRNA levels (Fig. 1D). Comparison of the expression of authentic fibrillar extracellular matrix (ECM) proteins showed that fibroblastic phenotypes demonstrated a fibrillar ECM staining pattern of fibronectin, while the normal phenotypes completely lost the staining potential of fibronectin (Fig. 2A). The protein expression level of fibronectin was more strongly upregulated in the fibroblastic phenotypes than in the normal phenotypes (Fig. 2B). Type I collagen produced by fibroblastic phenotypes demonstrated dual locations, at the ECM

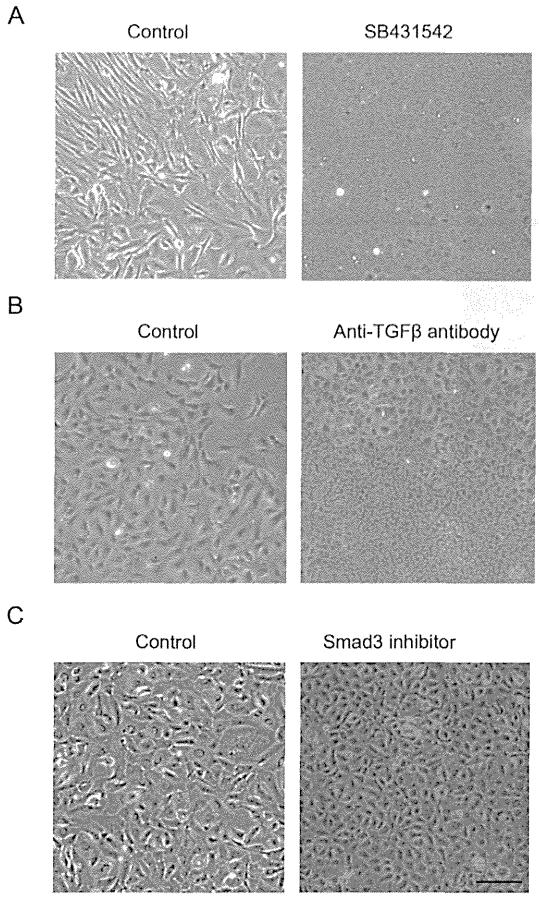

Figure 6. Inhibition of the TGFβ pathway suppressed the fibroblastic change of HCECs. (A) HCECs cultured with SB431542 (1 μM) exhibited the hexagonal cell shape and contact-inhibited monolayer, while the control CECs exhibited the fibroblastic morphology. (B+C) Both neutralizing antibody to TGF-β (500 ng/ml) and Smad3 inhibitor (3 mM) blocked cells from acquiring fibroblastic phenotypes. Scale bar: 50 μm. The experiment was performed in duplicate.
doi:10.1371/journal.pone.0058000.g006

and at the cytoplasm. Of interest, the cytoplasmic location of type I collagen appeared to be at the Golgi complex, the intracellular localization of which is essential for secretion, and these findings are similar to the published data [28]. On the other hand, type I collagen staining in the normal phenotypes was not clearly observed (Fig. 2A). RT-PCR analysis was used to determine the expression of major ECM proteins. The type I collagen transcript [α1(I) mRNA] was found to be abundantly expressed in the fibroblastic phenotypes, while the expression of α1(I) mRNA was negligible in the normal phenotypes (Fig. 2C). Unlike the type I collagen transcript, the basement membrane collagen phenotype α1(IV) mRNA was expressed in both the normal and fibroblastic phenotypes, yet to a lesser degree in the normal phenotype. Collagen phenotype α1(VIII) mRNA was expressed in both phenotypes at similar levels. Expression of fibronectin and integrin α5 was observed in the fibroblastic phenotypes, as opposed to the normal phenotypes in which the two transcripts were not expressed (Fig. 2C). On the other hand, β1 integrin mRNA was expressed in both phenotypes at similar levels (Fig. 2C).

Next, signaling pathways were determined to elucidate what might cause fibroblastic phenotypes of CECs. Since Smad2, p38, ERK1/2, and JNK are reportedly all involved in the EMT pathway [18–20,29,30], we therefore tested whether Smad2 and the MAPKs were involved in an endothelial-mesenchymal transformation similar to the EMT observed in epithelial cells (Fig. 3). Phosphorylation of Smad2 was found to be greatly promoted in the fibroblastic phenotypes when compared to that in the normal phenotypes. Phosphorylation of p38 and ERK1/2 was greatly enhanced in the fibroblastic phenotypes, while activation of JNK was negligible. These findings suggested that TGF-β signaling may exert the key role for the fibroblastic transformation of CECs.

TGF-β-mediated endothelial-mesenchymal transformation and use of TGF-β receptor inhibitor to block it in primate CECs

The findings shown in Fig. 3 led us to directly test whether SB431542, the TGF-β receptor inhibitor, was able to block the EMT process observed in the fibroblastic phenotypes. Phase contrast imaging demonstrated that primate CECs cultured in the presence of SB431542 exhibited the authentic polygonal cell shape and contact-inhibited monolayer, while the control CECs exhibited the fibroblastic morphology (Fig. 4A). Moreover, the SB431542-treated CECs showed the characteristic plasma membrane staining of Na^+/K^+-ATPase and ZO-1, while the control CECs lost their staining, suggesting that endothelial functions were maintained in the SB431542-treated cells (Fig. 4B). Furthermore, the expression of Na^+/K^+-ATPase and ZO-1 was strongly upregulated in the SB431542-treated fibroblastic phenotypes at both the protein (Fig. 4C) and mRNA levels (Fig. 4D). These data further confirmed that TGF-β might be the direct mediator of the endothelial to mesenchymal transformation observed in primate CEC cultures. Therefore, we tested whether the normal phenotypes were transformed to fibroblastic cells when exposed to the exogenous TGF-β, as in the findings shown in Fig. 5A. Of interest, the staining pattern of Na^+/K^+-ATPase and ZO-1 at the plasma membrane of the normal phenotypes was greatly reduced upon exposure of polygonal cells to TGF-β (Fig. 5B). The growth factor also markedly reduced the expression of the two proteins at protein levels in a concentration-dependent manner (Fig. 5C), while phosphorylation of Smad2 was greatly increased in a concentration-dependent manner (Fig. 5D). These data suggest that even the normal phenotypes of primate CECs are prone to acquire fibroblastic phenotypes in response to TGF-β-stimulation.

Two distinct phenotypes of HCEC cultures and the use of TGF-β receptor inhibitor to block endothelial-mesenchymal transformation

The interesting findings observed in primate CECs led us to further study whether HCECs were subjected to the similar undesirable prerequisite cellular changes leading to endothelial-mesenchymal transformation. Of great interest, cultivated HCECs lost the characteristic contact-inhibited monolayer and polygonal phenotypes, and acquired fibroblastic cell morphology like primate CECs (Fig. 6A). However, consistent with the primate CECs when the CECs were cultivated with the specific inhibitor to the TGF-β receptor (SB431542), the inhibitor was able to block alteration of the cell shape to fibroblastic phenotypes. Similar to the inhibitory effect of SB431542 on fibroblastic phenotypes, both neutralizing antibody to TGF-β (Fig. 6B) and Smad3 inhibitor (Fig. 6C) also blocked cells from acquiring fibroblastic phenotypes. We then tested whether SB431542 was able to maintain endothelial function. The findings shown in Fig. 7A and Fig. 7B demonstrated that blocking the TGF-β receptor signaling enabled the subcellular localization of Na^+/K^+-ATPase and ZO-1 at the plasma membrane and their protein expression to be maintained. Of

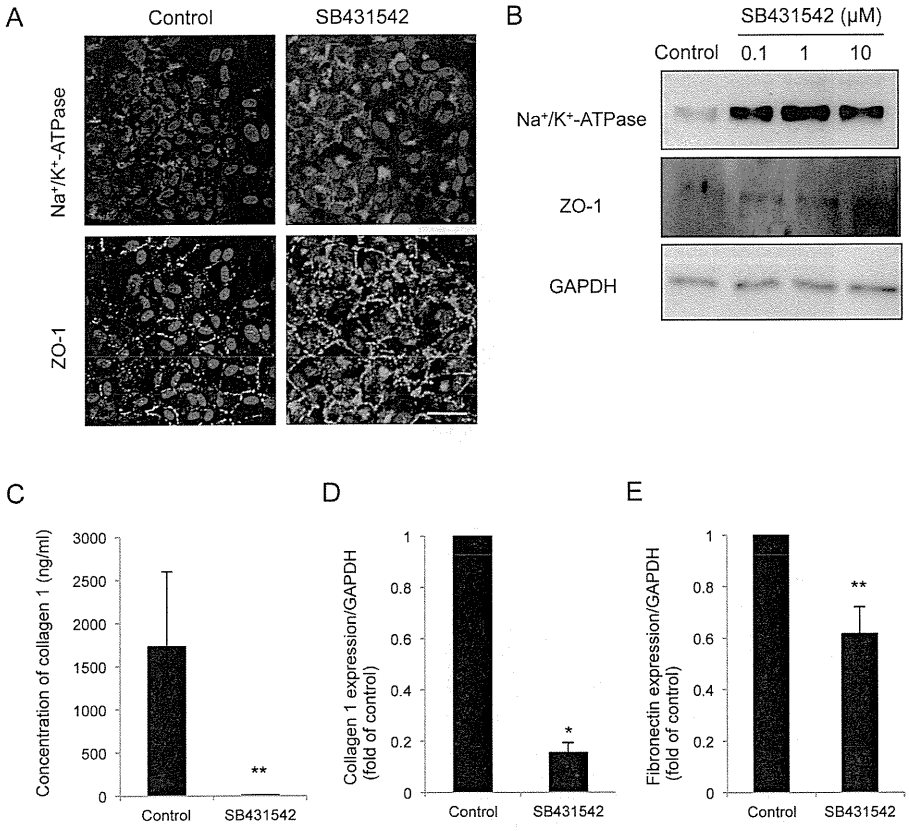

Figure 7. SB431542 maintained the functions and suppressed the fibroblastic change of HCECs. (A+B) Blocking the TGF-receptor signaling by SB431542 (A: 1 μM, B: 0.1, 1, and 10 μM) enabled the subcellular localization of Na^+/K^+-ATPase and ZO-1 at the plasma membrane and their protein expression to be maintained. Scale bar: 100 μm. (C) ELISA assay revealed that SB431542 significantly downregulated the secretion of type I collagen to the culture supernatant. **P<0.05. (D+E) Quantitative PCR showed that SB431542 significantly reduced the expression of type I collagen and fibronectin at the mRNA level. *$p<0.01$, ** $p<0.05$. Samples were prepared in duplicate. Immunoblotting, ELISA, and quantitative PCR were performed in duplicate.
doi:10.1371/journal.pone.0058000.g007

great importance, ELISA assay revealed that SB431542 markedly downregulated the secretion of type I collagen to the culture supernatant (Fig. 7C). Coincidentally, SB431542 markedly reduced the expression of type I collagen and fibronectin at the mRNA level (Fig. 7D, E).

Use of BMP-7 to suppress fibroblastic changes and maintain endothelial functions

Bone morphogenetic protein-7 (BMP-7) promotes MET and specifically inhibits the TGF-β-mediated epithelial-to-mesenchymal transition. Thus, that molecule has been used to antagonize the EMT process [31–34]. We therefore tested whether BMP-7 was able to antagonize the prerequisite changes of HCECs. The fibroblastic HCECs were treated with BMP-7 in a concentration ranging from 10 to 1000 ng/ml. Of important note, the elongated cell shapes of the fibroblastic phenotypes were reversed to the polygonal cell morphology in response to the presence of BMP-7 in a concentration-dependent manner (Fig. 8A). BMP-7 enabled the hexagonal cell morphology and actin cytoskeleton distribution at the cortex to be maintained (Fig. 8B), similar to that observed in normal CECs [35], and it also maintained the subcellular localization of Na^+/K^+-ATPase (Fig. 8C) and ZO-1 (Fig. 8D) at the plasma membrane. Thus, BMP-7 at the concentration of 1000 ng/ml was able to maintain CECs in polygonal and contact-inhibited phenotypes with a positive expression of function-related markers (Fig. 8E, F).

Discussion

Corneal endothelial dysfunction accompanied by visual disturbance is a major indication for corneal transplantation surgery [36,37]. Though corneal transplantation is widely performed for corneal endothelial dysfunction, researchers are currently seeking alternative methods to restore healthy corneal endothelium. The fact that corneal endothelium is cultured and stocked as 'master cells' from young donors allows for the transplantation of CECs with high functional ability and for an extended period of time. In addition, an HLA-matching transplantation to reduce the risk of rejection [38,39] and overcoming the shortage of donor corneas might be possible. Tissue bioengineering is a new approach to develop treatments for patients who have lost visual acuity [40]. To date, there are two methods that utilize bioengineering approaches: 1) use of cultured donor HCECs adhered on bioengineered constructs [4,5,7,9], and 2) transplantation of cultivated HCECs into the anterior chamber [11,41–43]. Regardless of which of the two methods is applied to clinical settings, establishment of an efficient cultivation technique for HCECs is essential and inevitable [44]. Many researchers have noticed that establishing a consistent long-term culture of HCECs is challenging [40]. Although the successful cultivation of HCECs has been reported by several groups, the procedures involved in the isolation and subsequent cultivation protocols varied greatly between laboratories [44]. One of the most difficult problems is

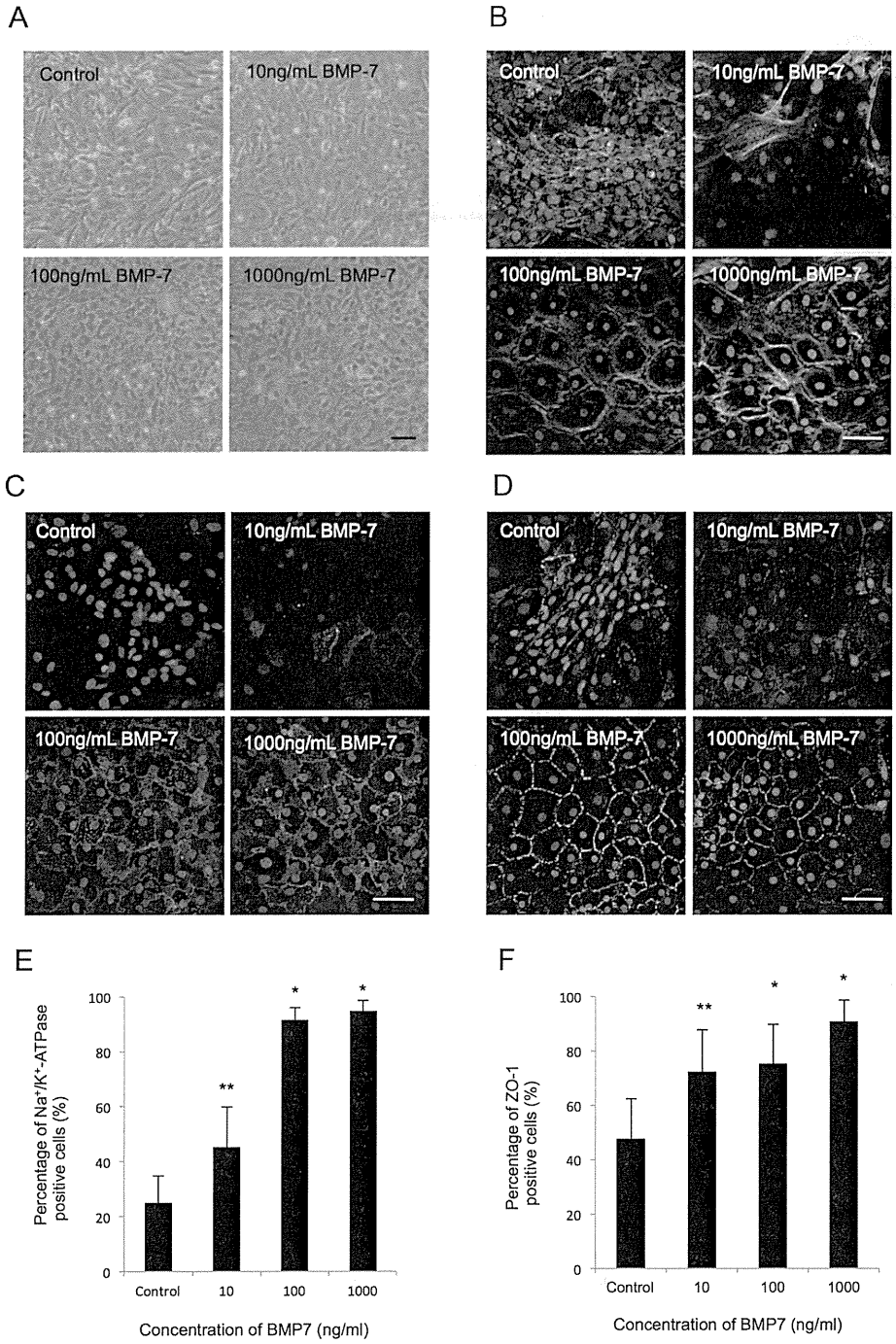

Figure 8. BMP7 suppressed fibroblastic change and maintained the functions of HCECs. (A) The elongated cell shapes of the fibroblastic phenotypes were reversed to a polygonal cell morphology in response to the presence of BMP-7 in a concentration-dependent manner. Scale bar: 50 μm. (B) BMP-7 enabled normal hexagonal cell morphology and actin cytoskeleton distribution at the cortex to be maintained. Scale bar: 100 μm. (C+D) BMP-7 maintained the subcellular localization of Na^+/K^+-ATPase and ZO-1at the plasma membrane. Scale bar: 100 μm. (E+F) The percentages of both Na^+/K^+-ATPase and ZO-1 positive cells treated with BMP-7 were significantly higher than in the control. * $p<0.01$, ** $p<0.05$. The experiment was performed in duplicate.
doi:10.1371/journal.pone.0058000.g008

that HCECs are vulnerable to undergoing massive fibroblastic change over each passage [40]. Therefore, it is essential to find means to circumvent the spontaneous transformation of the CECs in order to maintain the physiological phenotypes for the subsequent use for transplantation.

Transformation of endothelial cells to fibroblastic cells is designated as endothelial- mesenchymal transformation. Such transformation is triggered by TGF-β via the Smad2/3 pathway [16]. Endothelial-mesenchymal transformation causes the loss of the characteristic endothelial phenotypes, such as loss of the contact-inhibited monolayer and loss of the apical junctional

proteins at the plasma membrane. Furthermore, it causes induction of fibrillar proteins such as type I collagen and fibronectin. In this present study, we demonstrated that the fibroblastic phenotypes of cultivated CECs greatly lost the endothelial characteristics; expression of Na^+/K^+-ATPase and ZO-1 was markedly reduced and their subcellular localization was in the cytosol rather than the authentic plasma membrane location. Furthermore, fibroblastic phenotypes markedly enhance the production of fibrillar ECM proteins (type I collagen, fibronectin, and integrin α5) rather than basement membrane phenotypes (type IV and VIII collagens). The presence of such undesirable cells will greatly hamper the success of transplantation of cultivated cells in the clinical setting. Therefore, it is crucial to determine what causes the phenotypic changes and how to intervene in such endothelial-mesenchymal transformation processes of the cultivated CECs. The fact that phosphorylation of Smad2/3 was greatly enhanced in the fibroblastic phenotypes led us to conclude that the fibroblastic phenotypes in both primate and HCECs are mediated by TGF-β signaling. Therefore, we employed a specific inhibitor to the TGF-β receptor (SB431542) [45] to block the endothelial-mesenchymal transformation process observed in the fibroblastic phenotypes. SB431542 completely abolished the undesirable cellular changes, and when either primate or HCEC cultures were treated with SB431542, the prerequisite change of cells to fibroblastic phenotypes was completely abolished. Simultaneously, the characteristic subcellular location of ZO-1 and Na^+/K^+-ATPase is resumed at the plasma membrane and the expression of the two proteins is greatly increased at both mRNA and protein levels, suggesting that the barrier and pump functions in these cultures is intact. Moreover, we found that the production of fibrillar ECM proteins was greatly reduced. We further tested the effect of BMP-7, a well-known anti-EMT agent [31,34], to reverse the fibroblastic phenotypes of HCECs. BMP-7 also reversed the fibroblastic phenotypes to the normal endothelial cells with contact-inhibited monolayer and characteristic endothelial adhesion. Taken together, both SB431542 and BMP-7 can be powerful tools to maintain the normal endothelial phenotypes of the cultivated CECs, thus leading to a successful subsequent transplantation.

In conclusion, our findings showed that the use of the inhibitor to TGF-β receptor (SB431542) and/or anti-EMT molecules (BMP-7) enables HCECs to grow with maintaining normal physiological function (i.e., barrier and pump function). Although more extensive future studies would be beneficial, we have not observed any obvious adverse effects of continuous SB431542 or BMP-7 treatment on morphology and functions, even after several numbers of passages. This present study may prove to be the substantial protocol to provide the efficient *in vitro* expansion of HCECs. In addition, this novel strategy of inhibition of fibroblastic change during cultivation may ultimately provide clinicians with a new therapeutic modality in regenerative medicine, not only for the treatment of corneal endothelial dysfunctions, but also for a variety of pathological diseases in general.

Acknowledgments

The authors thank Dr. Morio Ueno, Dr. Michio Hagiya, Dr. Kiwamu Imagawa, Dr. Kenta Yamasaki, and Mr. Yuji Sakamoto for their valuable assistance with the experiments, and Mr. John Bush for reviewing the manuscript.

Author Contributions

Conceived and designed the experiments: NO EPK MN JH SK NK. Performed the experiments: NO MN. Analyzed the data: NO EPK MN JH SK NK. Contributed reagents/materials/analysis tools: NO SK NK. Wrote the paper: NO EPK NK.

References

1. Melles GR, Lander F, van Dooren BT, Pels E, Beekhuis WH (2000) Preliminary clinical results of posterior lamellar keratoplasty through a sclerocorneal pocket incision. Ophthalmology 107: 1850–1856; discussion 1857.
2. Price FW Jr, Price MO (2005) Descemet's stripping with endothelial keratoplasty in 50 eyes: a refractive neutral corneal transplant. J Refract Surg 21: 339–345.
3. Gorovoy MS (2006) Descemet-stripping automated endothelial keratoplasty. Cornea 25: 886–889.
4. Ishino Y, Sano Y, Nakamura T, Connon CJ, Rigby H, et al. (2004) Amniotic membrane as a carrier for cultivated human corneal endothelial cell transplantation. Invest Ophthalmol Vis Sci 45: 800–806.
5. Mimura T, Yamagami S, Yokoo S, Usui T, Tanaka K, et al. (2004) Cultured human corneal endothelial cell transplantation with a collagen sheet in a rabbit model. Invest Ophthalmol Vis Sci 45: 2992–2997.
6. Sumide T, Nishida K, Yamato M, Ide T, Hayashida Y, et al. (2006) Functional human corneal endothelial cell sheets harvested from temperature-responsive culture surfaces. FASEB J 20: 392–394.
7. Koizumi N, Sakamoto Y, Okumura N, Okahara N, Tsuchiya H, et al. (2007) Cultivated corneal endothelial cell sheet transplantation in a primate model. Invest Ophthalmol Vis Sci 48: 4519–4526.
8. Koizumi N, Sakamoto Y, Okumura N, Tsuchiya H, Torii R, et al. (2008) Cultivated corneal endothelial transplantation in a primate: possible future clinical application in corneal endothelial regenerative medicine. Cornea 27 Suppl 1: S48–55.
9. Koizumi N, Okumura N, Kinoshita S (2012) Development of new therapeutic modalities for corneal endothelial disease focused on the proliferation of corneal endothelial cells using animal models. Exp Eye Res 95: 60–67.
10. Okumura N, Ueno M, Koizumi N, Sakamoto Y, Hirata K, et al. (2009) Enhancement on primate corneal endothelial cell survival in vitro by a ROCK inhibitor. Invest Ophthalmol Vis Sci 50: 3680–3687.
11. Okumura N, Koizumi N, Ueno M, Sakamoto Y, Takahashi H, et al. (2012) ROCK inhibitor converts corneal endothelial cells into a phenotype capable of regenerating in vivo endothelial tissue. Am J Pathol 181: 268–277.
12. Miyata K, Drake J, Osakabe Y, Hosokawa Y, Hwang D, et al. (2001) Effect of donor age on morphologic variation of cultured human corneal endothelial cells. Cornea 20: 59–63.
13. Joyce NC, Zhu CC (2004) Human corneal endothelial cell proliferation: potential for use in regenerative medicine. Cornea 23: S8–S19.
14. Zavadil J, Bottinger EP (2005) TGF-beta and epithelial-to-mesenchymal transitions. Oncogene 24: 5764–5774.
15. Wendt MK, Allington TM, Schiemann WP (2009) Mechanisms of the epithelial-mesenchymal transition by TGF-beta. Future Oncol 5: 1145–1168.
16. Saika S (2006) TGFbeta pathobiology in the eye. Lab Invest 86: 106–115.
17. Kaimori A, Potter J, Kaimori JY, Wang C, Mezey E, et al. (2007) Transforming growth factor-beta1 induces an epithelial-to-mesenchymal transition state in mouse hepatocytes in vitro. J Biol Chem 282: 22089–22101.
18. Chen KH, Harris DL, Joyce NC (1999) TGF-beta2 in aqueous humor suppresses S-phase entry in cultured corneal endothelial cells. Invest Ophthalmol Vis Sci 40: 2513–2519.
19. Kim TY, Kim WI, Smith RE, Kay ED (2001) Role of p27(Kip1) in cAMP- and TGF-beta2-mediated antiproliferation in rabbit corneal endothelial cells. Invest Ophthalmol Vis Sci 42: 3142–3149.
20. Naumann GO, Schlotzer-Schrehardt U (2000) Keratopathy in pseudoexfoliation syndrome as a cause of corneal endothelial decompensation: a clinicopathologic study. Ophthalmology 107: 1111–1124.
21. Kawaguchi R, Saika S, Wakayama M, Ooshima A, Ohnishi Y, et al. (2001) Extracellular matrix components in a case of retrocorneal membrane associated with syphilitic interstitial keratitis. Cornea 20: 100–103.
22. Koizumi N, Suzuki T, Uno T, Chihara H, Shiraishi A, et al. (2008) Cytomegalovirus as an etiologic factor in corneal endotheliitis. Ophthalmology 115: 292–297 e293.
23. Song JS, Lee JG, Kay EP (2010) Induction of FGF-2 synthesis by IL-1beta in aqueous humor through P13-kinase and p38 in rabbit corneal endothelium. Invest Ophthalmol Vis Sci 51: 822–829.
24. Li W, Sabater AL, Chen YT, Hayashida Y, Chen SY, et al. (2007) A novel method of isolation, preservation, and expansion of human corneal endothelial cells. Invest Ophthalmol Vis Sci 48: 614–620.
25. Zhu C, Joyce NC (2004) Proliferative response of corneal endothelial cells from young and older donors. Invest Ophthalmol Vis Sci 45: 1743–1751.
26. Rheinwald JG, Green H (1975) Serial cultivation of strains of human epidermal keratinocytes: the formation of keratinizing colonies from single cells. Cell 6: 331–343.
27. Koizumi N, Fullwood NJ, Bairaktaris G, Inatomi T, Kinoshita S, et al. (2000) Cultivation of corneal epithelial cells on intact and denuded human amniotic membrane. Invest Ophthalmol Vis Sci 41: 2506–2513.